A STUDY OF THE INFLUENCE OF STRESS AND TEMPERATURE ON THE DAMPING CAPACITY OF MN-CU ALLOYS FOR SHIP SILENCING APPLICATIONS

Norman Anthony Hills

NAVAL POSTGRADUATE SCHOOL
Monterey, California

THESIS

A Study of the Influence of Stress and Temperature on the Damping Capacity of Mn-Cu Alloys for Ship Silencing Applications

by

Norman Anthony Hills

September 1974

Thesis Advisor: Glen Edwards

UNCLASSIFIED

SECURITY CLASSIFICATION OF THIS PAGE (When Date Entered)

REPORT DOCUMENTATION PAGE		READ INSTRUCTIONS BEFORE COMPLETING FORM
1. REPORT NUMBER	2. GOVT ACCESSION NO.	3. RECIPIENT'S CATALOG NUMBER
4. TITLE (and Subtitle) A Study of the Influence of Stress and Temperature on the Damping Capacity of Mn-Cu Alloys for Ship Silencing Applications		5. TYPE OF REPORT & PERIOD COVERED Mechanical Engineer; September 1974 6. PERFORMING ORG. REPORT NUMBER
7. AUTHOR(s) Norman Anthony Hills		8. CONTRACT OR GRANT NUMBER(s)
9. PERFORMING ORGANIZATION NAME AND ADDRESS Naval Postgraduate School Monterey, California 93940		10. PROGRAM ELEMENT, PROJECT, TASK AREA & WORK UNIT NUMBERS
11. CONTROLLING OFFICE NAME AND ADDRESS Naval Postgraduate School Monterey, California 93940		12. REPORT DATE September 1974 13. NUMBER OF PAGES 102
14. MONITORING AGENCY NAME & ADDRESS(if different from Controlling Office) Naval Postgraduate School Monterey, California 93940		15. SECURITY CLASS. (of this report) Unclassified 15a. DECLASSIFICATION/DOWNGRADING SCHEDULE

16. DISTRIBUTION STATEMENT (of this Report)

Approved for public release; distribution unlimited

17. DISTRIBUTION STATEMENT (of the abstract entered in Block 20, if different from Report)

18. SUPPLEMENTARY NOTES

19. KEY WORDS (Continue on reverse side if necessary and identify by block number)

Manganese-Copper alloys
Incramute
Damping Capacity
Sonoston
Ship silencing
Fatigue
Stress effect on damping capacity

20. ABSTRACT (Continue on reverse side if necessary and identify by block number)

Mn-Cu alloys develop a high damping capacity after a heat treatment of aging and subsequent quenching. The damping capacity developed is extremely sensitive to aging time at a given temperature or temperature for a fixed time. The optimum heat treatment developed for the commercial alloy Incramute was: 1) a 30 minute solutioning in the single phase γ_{Mn} region, 2) a water quench, 3) an 8 hour age at 400°C, and 4) a water quench to ambient

DD FORM 1 JAN 73 1473 EDITION OF 1 NOV 65 IS OBSOLETE
S/N 0102-014-6601 |
(Page 1)

UNCLASSIFIED

SECURITY CLASSIFICATION OF THIS PAGE (When Date Entered)

20. Abstract

temperature.

The effect of stress applied during the heat treatment of Incramute is significant. A tensile load precludes the development of high damping capacity for the aging times investigated (up to 50 hours in some cases). A compressive load only increases the time required to achieve the maximum damping capacity. A preliminary study of the effect of stress applied during heat treatment of Incramute indicates that the major disruption to development of high damping capacity occurs during the aging portion of the heat treatment.

An endurance limit of 29,000 psi can be expected for Incramute aged to its maximum damping condition.

A Study of the Influence of Stress and Temperature on the Damping Capacity of Mn-Cu Alloys for Ship Silencing Applications

by

Norman Anthony Hills
Lieutenant, United States Navy
B.S., Cornell University, 1967

Submitted in partial fulfillment of the
requirements for the degree of

MECHANICAL ENGINEER

from the

NAVAL POSTGRADUATE SCHOOL
September 1974

ABSTRACT

Mn-Cu alloys develop a high damping capacity after a heat treatment of aging and subsequent quenching. The damping capacity developed is extremely sensitive to aging time at a given temperature or temperature for a fixed time. The optimum heat treatment developed for the commercial alloy Incramute was: 1) a 30 minute solutioning in the single phase γ_{Mn} region, 2) a water quench, 3) an 8 hour age at 400°C, and 4) a water quench to ambient temperature.

The effect of stress applied during the heat treatment of Incramute is significant. A tensile load precludes the development of high damping capacity for the aging times investigated (up to 50 hours in some cases). A compressive load only increases the time required to achieve the maximum damping capacity. A preliminary study of the effect of stress applied during heat treatment of Incramute indicates that the major disruption to development of high damping capacity occurs during the aging portion of the heat treatment.

An endurance limit of 29,000 psi can be expected for Incramute aged to its maximum damping condition.

TABLE OF CONTENTS

LIST OF TABLES

LIST OF FIGURES

TABLE OF SYMBOLS AND ABBREVIATIONS

A1	Amplitude of first torsional vibration
A2	Amplitude of second torsional vibration
c	Specimen radius
d	Specimen diameter
D	Diameter of inertia disk
FCC	Face centered cubic
FCT	Face centered tetragonal
J	Centroidal polar moment of inertia
S.D.C.	Specific damping capacity
S_s	Shear stress
T	Torque
W	Applied force due to dead weights
Y.S.	Yield stress
ω_A	Uncertainty in A1
ω_B	Uncertainty in A2
ω_c	Uncertainty in specimen radius
ω_s	Uncertainty in S.D.C.
ω_{ss}	Uncertainty in shear stress
ω_T	Uncertainty in torque
ω_J	Uncertainty in polar moment of inertia
ω_W	Uncertainty in weight of the dead weights
OSHA	Occupational Safety and Health Administration
ω_r	Uncertainty in fatigue specimen radius

ω_l	Uncertainty in lever arm of R.R. Moore fatigue machine
S	Stress
r	Specimen radius
M_s	Temperature at which martensite starts to form
M_f	Temperature at which martensite stops forming
M_d	Temperature of stress induced martensite
a_t	Cell dimension in the tetragonal state
c_t	Unequal cell dimension in the tetragonal state
a_c	Length of cell side in the cubic state
psi	Pounds force per square inch

ACKNOWLEDGEMENT

I am extremely grateful to Mr. Roy Edwards. Without his time, skill and experience this project would have been a much more difficult and less productive task.

I. INTRODUCTION

A. GENERAL

Ship silencing has long been an important aspect of submarine design and construction. It is becoming the single most important requirement in new and future construction. Quietness is important for two reasons. First, in order to remain undetected by passive listening sonars, the submarine must be more quiet than the background ambient noise in which it is operating. Secondly, to take advantage of itself as a superior sonar platform, a submarine must not produce any noise or vibration that would detract from its capability to discriminate a contact from the background noise.

Other areas of ship construction and construction, both military and civilian, are also becoming aware of the need for sound silencing. One manifestation of this is the continuing noise level requirements legislated by the Occupational Safety and Health Administration (OSHA). Because of these various reasons there is a mushrooming industry concerned with methods of sound silencing and vibration control.

B. VIBRATION CONTROL

Vibration control consists of two schemes:

1. Isolation, i.e. prevention of energy transmission between the source and the surfaces that radiate the sound and vibration.

2. Dissipation or attenuation of the energy somewhere within the structure.

To date, the major engineering effort has been in developing methods to be used on existing machinery and structures. The methods can be classified as:

1. Isolation of the source of excitation from the structure by means of some sort of viscoelastic mount.

2. Blanketing to minimize radiated noise.

3. Increasing the stiffness of the offending source to minimize the amplitude of forced vibration.

4. Tuning to avoid resonances.

5. Decreasing manufacturing tolerances in an effort to reduce noise and vibration sources.

These are only remedial solutions which address the problem after the fact.

The Navy's main effort has been in the area of isolation. Resilient mounting of machinery to reduce transmitted vibrations and noise is the method generally accepted. However, unlike shore-mounted machinery, shipboard machinery must also withstand shock loadings due to general operating requirements and the possibility of hostile action. A resilient mount that can be optimally chosen to reduce transmitted machinery vibration would not be optimum for shock isolation and vice versa. As a result, the mounts which are presently used are a compromise of both requirements.

The only effort to control vibration by dissipation within the structure has been the use of cast iron in the

design of machinery. Cast iron has unconciously been accepted as the only available structural material with significant internal damping; however, Figure 1 indicates that there are higher damping materials available. Of interest here are the Manganese-Copper alloys, two of which are now available commercially.

C. MANGANESE-COPPER ALLOYS

The fact that Mn-Cu alloys can have a high damping capacity has been known for many years. Dean [1,2] is probably the first person to investigate in depth the damping capacity of Mn-Cu alloys. This work at the U.S. Bureau of Mines at Rolla, Missouri was continued by Jensen [3]. In the late 1960's there was a great proliferation of published research on these alloys primarily from England, the United States and the Soviet Union.

The high damping capacity of the Mn-Cu alloys has intrigued naval architects since its discovery. The primary consideration was for use in marine propellers [4-10]. In earlier reports, the alloys were found physically unsatisfactory because of poor quality castings. More advanced alloys tested in later reports were physically sound but still susceptible to general corrosion and stress corrosion cracking in salt solution. For these reasons they were deemed unsatisfactory for use in marine propellers. However these results may not be universally applicable [11].

In one instance [12] a Mn-Cu alloy was considered for use in marine propulsion gears. Again, because of inclusions

and flaws, the material was found to be physically unfit for use.

D. PHYSICAL METALLURGY OF MANGANESE-COPPER ALLOYS

The Mn-Cu binary phase diagram is shown in Figure 2. High damping is associated with alloys of greater than about 20% Mn; practical alloys range from about 70Cu-30Mn to 30Cu-70Mn. These alloys must be subjected to four heat-treatment steps in order to obtain high damping properties:

1. Solution treatment in the (γ_{Mn}) single phase region (face centered cubic structure).

2. Room temperature quench to preserve the single phase metastable supersaturated solid solution produced by treatment 1.

3. An aging treatment (approximately 8 hours at 400°C) in the two phase ($\gamma_{Mn} + \alpha_{Mn}$) region. Aging is a diffusional process which apparently produces metastable zones of Mn enrichment prior to precipitation of α_{Mn}, the equilibrium precipitate. Underaging or overaging will result in inferior damping properties due to insufficient conditioning and excessive α_{Mn} precipitation respectively [13,14].

4. A room temperature quench. During this quench, antiferromagnetic ordering occurs at a specific temperature, the Néel temperature (T_N), the structure distorting to face centered tetragonal as this ordering occurs. Ordering assists a martensitic transformation which occurs on cooling through the martensitic transformation temperature range (Figure 4), a martensitic structure is characterized by submicroscopic domains of complimentary orientation [13,15].

The high damping capacity can be attributed to motion of the domain boundaries. Under cyclic elastic loads, energy absorption takes place by the oscillation of the domain boundaries, resulting in a macromechanical hysteresis effect. The process is mechanically (though not thermodynamically) reversible and is not associated with appreciable increases in the density of dislocations or other crystalline imperfections.

Some work [3,16] has been done on the effect of third elements on the Mn-Cu system. There are varying effects due to the added element depending on the amount added. However no addition increases the damping capacity, most reduce it. Amounts of carbon and silicon greater than 0.2% severly reduce damping capacity in Mn-Cu alloys. Dean [17] did extensive work on the Cu-Mn-Al system. Figure 3 indicates the effect of Al on the Mn-Cu system at the optimum damping temperature.

A primary problem with unlimited application of Mn-Cu alloys is the temperature dependence of their damping capacity (Figure 5). The damping capacity decreases with increasing temperature, undergoing significant change as it heats through the reverse transformation. The curve on Figure 5 which does not drop off until approximately 80°C was reported by the American Potash and Chemical Corporation [18]. This is a result of research that included the addition of vanadium to Mn-Cu alloys. Although the overall damping capacity for this Cu-Mn-Al alloy is less than that

of other Mn-Cu alloys, it is still significantly better than most structural materials (Figure 1) and the improved temperature range makes this alloy promising. Increasing the temperature range of high-damping-capacity alloys is an important metallurgical challenge.

II. OBJECTIVES

A. MATERIALS

Mn-Cu alloys of high damping capacity are just now becoming commercially available and are difficult to obtain in small research quantities. Accordingly, these priorities were taken:

1. Locate and obtain any commercially available Mn-Cu alloys.

2. Manufacture various binary Mn-Cu alloys in the laboratory in lieu of commercially available alloys. If commercial alloys are obtained, then the binary alloys would be used as a comparison to see what improvements, if any, the commercial alloys afford.

B. GRAIN GROWTH AND RECRYSTALLIZATION

To determine the material response to thermomechanical treatment, it was decided that the first tests should be a standard series of grain growth and recrystallization tests. This would allow the estimation of the time required at given temperatures to create various grain sizes and shapes, as well as vary the deformation substructure. This information was desired for several reasons. First, these metallurgical features could be varied and the associated damping response determined. It was also important that the simultaneous aging-recrystallization kinetics be known during aging trials.

C. STRESS DEPENDENCE

As a result of the face centered cubic (FCC) to face centered tetragonal (FCT) transition, the high damping phase has an asymmetric configuration. Each grain has an associated c direction. The c/a ratio [13,15,19] is dependent on aging time, aging temperature, and composition (Figures 6,7). It has been pointed out that since the c/a ratio is less than 1, application of compressive stress to a single crystal will favor the FCT c-axis parallel to the stress direction while tensile stress will favor the FCT c-axis perpendicular to the stress direction [13,15]. When an elastic compressive stress is applied to the material, domains with their c-axis most nearly parallel to the axis of compression will be nucleated or grow at the expense of domains less favorably oriented. When the stress is released the domains will shrink back anelastically to their original positions.

The martensitic structures formed in Mn-Cu alloys are very likely of the low hysteresis, thermelastic type commonly observed in shape-memory effect alloys [20]. Such martensites are extremely sensitive to stress and temperature in their formation. In general, whether during stress-induced transformation or deformation, these martensites respond to stress in such a way as to best relieve that applied stress. This means that certain orientation varients, specific transformation shears, etc. are favored over others.

In single crystals it may be that the stress for stress-induced martensite formation is orientation dependent.

When a polycrystalline "austenitic" alloy, properly conditioned (by aging) for martensitic transformation, is cooled through the Néel temperature, each austenitic grain will transform from FCC to FCT during antiferromagnetic ordering. Each grain will adopt a c-axis direction, and the overall arrangement of c-axis directions will be such as to provide greatest total accomodation in the material for the local elastic stresses created by the transformation. In the absence of external loading, the c-axis directions would be expected to be randomly oriented in space. Application of an external load during the transformation should create a preferential orientation for the c-axis. The result should be the formation of a preferred crystallographic orientation from which martensite will form when cooled through M_s. The magnitude of the load will also affect the array of martensite plate orientation varients formed within the FCT grains.

One of the objectives of this investigation is to determine if the martensite plate orientation can be controlled by the application of an external load during the aging and/or quenching phase of the heat treatment with the result that the S.D.C. in a given direction in the sample could be likewise controlled.

D. FATIGUE

The fatigue resistance of Mn-Cu alloys has not been well characterized in spite of the fact that this metallurgical system is best applied to designs associated with vibration. Specifically, there have been only two [3,21] published reports that investigate the fatigue properties of Mn-Cu alloys. Both studies considered only binary Mn-Cu systems.

Because of the high internal damping, a significant amount of energy associated with a cyclic stress will be transformed into heat by the damping process. The relatively low thermal conductivity of the material can be expected to result in high specimen temperatures. As the temperature increases, the specimen damping capacity will decrease, thus producing a self-limiting cycle. In fact the temperatures caused should be sufficient to age the material thus resulting in a lower damping capacity due to overaging [14, 21,22].

One of the objectives of this investigation was to characterize the stress-life to failure (S-N) behavior of the commercial alloy "Incramute" by the classic rotating bending technique. After failure, the fracture surfaces of several of the specimens could be examined using a scanning electron microscope (SEM).

III. EXPERIMENTAL METHODS

A. MATERIAL

At present there are two primary suppliers of Mn-Cu based high damping alloys. An alloy known as "Sonoston" (nominally 37 Cu, 54.25 Mn, 4.25 Al, 3 Fe, 1.5 Ni) is produced by Stone Manganese Marine Ltd., London, while "Incramute" (nominally 58 Cu, 40 Mn, 2 Al) is marketed through INCRA (International Copper Research Association), New York. Both organizations graciously contributed sample material for this study. In addition, NSRDC, Annapolis, Maryland, supplied quantities of excess "Sonoston" alloy from earlier studies in that laboratory [9].

B. RECRYSTALLIZATION AND GRAIN GROWTH TRIALS

Both of the commercial Mn-Cu base alloys mentioned above were solution treated by heating to 800°C for thirty minutes and then water quenching. Samples were cold-worked by rolling 5, 10, 30, 50 and 70% of the original thickness. One sample of each thickness reduction was annealed for thirty minutes at six different temperatures over the temperature range 400°C to 800°C.

C. METALLOGRAPHY

All metallographic specimens were prepared as follows:

1. Sand on 0 grit emery paper
2. Sand on 3/0 grit emery paper

3. Polish on 3 micron diamond dust wheel

4. Polish on 1 micron diamond dust wheel

5. Polish on .05 micron alumina wheel

6. Ferric chloride etch (100 ml. Ethanol, 5 gm. FeCl, 2 ml. HCl)

Photomicrographs were taken with a Zeiss photomicroscope with automatic exposure device.

D. TENSION STRESS-AGE-QUENCH (TSAQ) APPARATUS

A BLH Baldwin creep-rupture testing machine was modified to allow aging and quenching of torsion pendulum specimens while under stress. A Marshall Tube Furnace was arranged vertically with a thin-wall steel tube placed inside (Figure 8). This arrangement allowed the specimens to be aged and quenched in the furnace with simultaneous stress application.

The two basic aging procedures were employed initially. One of these involved loading a certain percentage of the yield stress during the entire aging period, followed by quenching with or without stress. A second scheme involved application of zero stress until the end of the aging period at which time the specimen was loaded and immediately quenched.

E. COMPRESSION STRESS-AGE-QUENCH (CSAQ) APPARATUS

A compression apparatus (Figure 9) was manufactured to hold the same specimens at the TSAQ apparatus. The load was applied by placing weights on the top of the upper loading head. The whole apparatus fit inside a Marshall Tube

Furnace (Figure 10). The same aging procedures used in the TSAQ apparatus were repeated. The specimen was quenched by removing the entire apparatus from the furnace and placing it in a large can of water.

F. DAMPING CAPACITY MEASUREMENT

A torsional pendulum originally built and used by the U.S. Bureau of Mines, Rolla, Missouri was obtained from NSRDC, Annapolis, Maryland (Figure 11).

The specimens were bars seven inches long with a five inch test section machined to .200 inch diameter. The torsional vibration amplitude was measured by a strain gage mounted on the specimen (Figure 12). The strain gage output was amplified and visually presented by a Honeywell Visicorder (Figure 13). Calibration was accomplished by application of known torsional moments by means of a string-weight-pulley system. Torsion pendulum operating frequency was 4-5 Hz.

The specific damping capacity (S.D.C.) was calculated from:

$$S.D.C. = \left(\frac{A1^2 - A2^2}{A1^2} \right) \quad 100$$

where A1 and A2 represent the amplitudes of successive vibration peaks. For each specimen the S.D.C. was measured at a surface shear stress of 1,000, 5,000, 10,000 psi.

G. FATIGUE TESTS

A plate of the as-received Incramute was solutioned 2 hours at 720°C, then cold rolled to a 50% reduction in thickness. Specimens for an R.R. Moore high speed (10,000 rpm) fatigue machine were then machined from the material (Figure 14). Machined specimens were resolutioned at 720°C for 30 minutes, then aged 8 hours at 400°C to obtain maximum damping capacity.

No effort was made to keep the specimen surface uncontaminated. The surface was not cleaned after the heat treating operations. The result was a specimen with a surface roughness of 32 on a General Electric surface roughness scale.

IV. RESULTS AND DISCUSSION

Because of the availability of commercial alloys, it was decided not to attempt to make binary alloys as part of this program. With the exception of the recrystallization and grain growth trials, all tests were conducted exclusively with "Incramute".

A. RECRYSTALLIZATION AND GRAIN GROWTH

Typically, the effect of prior cold work on recrystallization response results in a set of curves such as shown schematically in Figure 15. The experimental curves for Sonoston (Figure 16) and Incramute (Figure 17) differ from this typical behavior due apparently to the superposition (in some cases) of an age-hardening response on the expected softening effects of recovery, recrystallization, and grain growth. This was not unexpected since the annealing temperatures were within a two-phase field.

A very unusual annealing behavior for the alloys is illustrated by Figure 16 in which the recrystallization temperature apparently increases with increasing prior cold work in contrast from the usual inverse relationship between recrystallization temperature and prior cold work. From this one might conclude that more thermal energy is necessary to initiate the atomic rearrangements of recrystallization for larger amounts of cold work which is not sensible. It

is believed that this unusual response must be due to the effect of simultaneous precipitation (strengthening) processes in the alloys during the annealing periods. This type of effect is more clearly defined for the "Incramute" annealing curves (Figure 17).

B. AGING EFFECTS ON DAMPING CAPACITY

It was found in early aging tests that the standard aging program recommended by INCRA [23] (400°C for nine hours per inch of section thickness) must not be literally interpreted. Standard torsion pendulum samples (0.2 inches in diameter) were aged eight hours at 400°C before maximum damping capacity was attained (Figures 18, 19, 20). Aging at temperatures lower than 400°C increases the time-to-maximum-damping significantly. Aging at higher temperatures reduces the maximum S.D.C. achievable. Figure 21 illustrates this and also indicates that it may be possible to achieve higher damping capacities at aging temperatures below 400°C if one is willing to accept the time penalty. All the curves in Figure 21 are the result of single sample experiments with the exception of the 400°C curve. This strong temperature dependence is probably indicative of a diffusional process that is being accelerated at the higher temperatures and operating with difficulty at the lower temperature.

It is obvious that the S.D.C. that can be developed is significant, in one case 57% at 10,000 psi surface shear stress. The Mn-Cu alloys are in fact in the position

indicated in Figure 1. Figure 22 shows the characteristic torsion pendulum outputs for "Incramute" in the aged (high damping) condition versus the low damping solutioned form.

Because of physical limitations of the torsion pendulum, some aged specimens could not be twisted enough to obtain 10,000 psi surface shear stress, as they became quite "rubbery" after conditioning by aging and quenching [1, 3, 19]. Those specimens which demonstrated this behavior exhibited high damping. The behavior indicated an apparent change in the shear modulus with aging. The general trend was for the modulus to apparently decrease with aging time at a given temperature, then increase again.

Briefly summarized, specimens with optimum conditioning by aging (for high S.D.C.) would be most highly martensitic; the martensitic structure reflects an apparently lower modulus (rubbery behavior) for the material under stress because of recoverable deformation mechanisms that are not truly elastic. This is typical of so-called thermoelastic martensites found in shape memory effect alloys [20].

It has been reported that for the binary Mn-Cu system there is approximately 0.6% linear shrinkage with aging [24, 25]. In this study sample length was monitored during aging. Machined "Incramute" torsion pendulum samples were observed to shrink when the as-received plate material was re-aged after re-solutioning. Shrinkage of 0.3% to 0.5% was observed to occur early in the aging process before any significant damping capacity was developed. This agrees

well with the data reported by Jensen and Walsh [3]. The early shrinkage is supported by previously reported results [19]. Such shrinkage was also observed in a sample stress-aged while axially loaded in tension to 60% of the yield stress.

C. STRESS EFFECTS DURING AGING AND/OR QUENCHING ON DAMPING CAPACITY

Table I gives the results of the tensile (TSAQ) tests conducted by applying an elastic stress during age and/or quench. The value of the yield strength used is 38,000 psi [24]. Because of low S.D.C.'s and to conserve expensive strain gages, only a few tensile specimens were tested in the torsional pendulum. The S.D.C. figures were qualitatively determined by comparing the "ring" of the specimen when dropped on a concrete floor with that of a solutioned specimen (1.1%, 1.0%, 1.8% at 1,000, 5,000, 10,000 psi respectively).

The results can be summarized:

1. Application of uniaxial tension stress (.09% Y.S. to 60% Y.S.) during aging and quenching results in the development of no significant damping for aging times from 15 minutes to 50 hours at 400°C.

2. Application of 4.94% Y.S. uniaxial tensile stress only during the aging treatment produces no significant damping for aging times from 0.5 hours to 10 hours at 400°C. (Note: stress equivalent to 0.09% Y.S. from the lower grip weight applied during quench)

3. Application of 4.94% Y.S. uniaxial tensile stress during the quench only (after aging 8 hours at 400°C) produces no significant damping capacity. (Note: stress equivalent to 0.09% Y.S. from the lower grip weight applied during age)

Compression retarded the time required to achieve maximum S.D.C. but did not seem to affect the maximum S.D.C. that could be obtained. Four different series of tests were run. The first three test series utilized the same loading, but the load was applied during different stages of the conditioning process. The object was to attempt to segregate the stress effect into:

1. The effect of stress on the aging process.

2. The effect of stress on the quenching process.

The fourth series was to determine the effect of varying the magnitude of the stress during heat treatment.

The results, seen in Figures 23, 24, 25, can be summarized:

1. As with the tension tests, limited data imply that the compressive stress affects both the aging process and the quenching process, unless a stress as low as .09% Y.S. affects aging.

2. The greater the shear stress, the longer the time required to achieve maximum S.D.C. However, the average maximum S.D.C. attained corresponds well to the 400°C curve in Figure 21.

3. Three of the four 1,000 psi curves exhibit an ability to regain significant S.D.C. after apparently passing the maximum and beginning to decrease.

Comparing the maximum S.D.C. obtained in these tests with that of Figure 21 (see Figure 26) it is apparent that there isn't much difference. Although two of the curves aren't complete, it appears that, except for 1,000 psi, there is a certain maximum value to be associated with each surface shear stress.

The results of the tension (TSAQ) and compression (CSAQ) tests are summarized in Figure 27. The maximum S.D.C.'s plotted were those obtained in the tests regardless of the time required to obtain them. (Note: the maximum time considered was 50 hours)

Because there is no clear indication that the application of stress, tensile or compressive, preferentially effects the aging or quenching process, the possible effects during each process must be considered.

1. Stress Effect on the Aging Process

The apparent reactions [26] which occur during aging of Mn-Cu alloys are summarized in Figure 28. Aging is an essential step in the heat treating process because it conditions the matrix for the martensitic transition that occurs on subsequent quenching. The martensitic structure is responsible for the high damping capacity so the damping capacity is a direct measure of the success of previous heat treatment.

The aging process is a diffusional process. However, the effect of elastic stress on diffusional nucleation and growth processes is not clearly established. Reports indicate that stress can sometimes accelerate and in other cases retard diffusional nucleation and growth reactions. In fact, in some systems, stress may retard in one circumstance and accelerate in another. The important variables are stress level and temperature.

Relevant observations can be made from the AL - 4Cu age hardening system. Resolution of stable (Θ) precipitates under stress-aging conditions has been reported [27]. In alloys of Al-4Cu, the activation energy of dissolution of the Θ precipitate decreases from 70 kcal/mole without stress to 40 kcal/mole with a stress of only 200 psi. In another study [28] of the same alloy system, the activation energy for aging with stress (1,000 psi) was 29.75 kcal/mole as opposed to 28.5 kcal/mole without stress. These values do not correspond to that for diffusion of Cu in Al or for Al self-diffusion indicating that diffusion is not the rate controlling process. The rate controlling reaction in this case is a volume contraction of approximately 5%.

Thus a tensile stress during age can both accentuate [27] and retard [28] a precipitation reaction. Many of the observed effects of stress on aging reactions have been explained by versions of the "Bilby volume change criterion". This is based on the restraint of inherent volume changes for the structural phase change involved. In reference 28

it appears that the tension opposing a volumetric contraction explains the retarding of the overall reaction kinetics. This may in fact be what is happening during the compression and tension tests. The tensile specimens shrank .38% on the average while the compressive specimens shrank .47% on the average.

Returning to Figure 29, the effect of tensile stress during aging in eliminating damping may be to:

a. Accelerate the $\gamma_{Mn} \rightarrow \alpha_{Mn}$ reaction, or

b. Retard of eliminate the $\gamma_{Mn} \rightarrow$ "ω" reaction.

If, for example, the α reaction is accelerated by tensile stress or if the "ω" reaction is slowed down, the reaction may dominate the aging response resulting in no matrix conditioning and therefore low damping.

2. Stress Effect on the Quenching Process

The quenching process is required to cool the specimen through the martensitic transformation temperature range. A martensitic transformation may be induced either by cooling or by application of stress. The shear stress necessary to cause martensitic transformation is zero at M_s and increases with temperature above M_s until another critical temperature, M_d, is reached. Above M_d, the stress will be manifested as classical slip deformation of the high temperature phase, rather than by shear transformation.

In a martensitic transformation, the major portion of the critical driving force may correspond to work required for the transformation shear and accomodation strains. The

required work increment for transformation shears and accomodation does influence the free energy change required for the reaction to occur and therefore affects the phase stability ranges. The thermal contribution to the free energy change at any temperature can be expressed as:

$$D_{A\rightarrow M} = \Delta F_{A\rightarrow M} + U_{A\rightarrow M}$$

where $\Delta F_{A\rightarrow M}$ is the thermal contribution to the free energy change under conditions of zero stress, and U is the stress contribution to the free energy change at temperature T.

The role of the applied stress can be determined from:

$$U = \tau \gamma_o + \sigma_N \epsilon_N$$

where τ is the resolved shear stress along the habit plane; γ_o is the transformation shear strain; σ_N is the normal stress resolved perpendicular to the habit plane; ϵ_N is the normal component of the transformation strain. Since the habit plane is an invarient plane, $\epsilon_N = \Delta V$. Thus the sign of ϵ_N is negative for an overall transformation contraction, positive for expansion. When the normal stress is tensile, σ_N is numerically positive, and negative when the normal stress is compressive. Because the many habit permutations permit shearing in either sense, τ is taken to be positive. Depending on the sign of ϵ_N and σ_N, the transformation may be either assisted or opposed by the normal component.

Patel and Cohen (29) have shown, for Fe-Ni and Fe-Ni-C alloys, which have a positive ϵ_N, that M_s is raised by uniaxial tension, raised to a lesser extent by uniaxial compression and lowered by hydrostatic pressure.

Available lattice parameter data for certain Mn-Cu alloys (13,15) may be used to approximate ΔV where ΔV is defined as:

$$\Delta V = \frac{a_t^2 c_t - a_c^3}{a_c^3}$$

From Figure 6; a_t=3.75, a_c = 3.75, c_t = 3.71. Therefore ΔV = -0.01 or approximately 1% contraction for the cubic (c) to tetragonal (t) reaction. The value ΔV is identically equal to ϵ_N; i.e. $\epsilon_N \simeq -0.01$. Because the sign of is negative for compressive stress, the result is that U must be positive; i.e. compressive stress during quench should cause the martensitic transformation in Mn-Cu alloys to occur at an M_s temperature higher than the normal M_s. Furthermore, the martensitic transformation should be more favored by compressive stresses than by tensile stresses. Conversely a tensile stress would increase M_s to a lesser extent or lower it depending on the precise magnitude of ΔV.

Thus a specimen quenched under a compressive stress would be expected to transform at a higher temperature and exhibit high damping capacity at room temperature after the stress is removed, which it does. A specimen quenched under a tensile stress may or may not exhibit high damping at room

temperature while still under stress, depending on the extent to which the $\sigma_N \epsilon_N$ term affects the sign of U . However, when the stress was removed the transformation should then take place. This was not the experimental result observed; samples of the tensile stress test series which supposedly had been properly conditioned by aging exhibited no significant damping capacity after the quenching stress was removed.

A plausible explanation for an apparent stress-quenching effect might be that subtle irreversible microstructural changes occur when the martensitic transformation is suppressed by an applied stress so that even when the stress is removed, a transformation which would ordinarily be spontaneous does not occur. The fact that quenching stresses of only 3 or 6% Y.S. produced these results is difficult to believe.

The alternate conclusion is that 34 psi (created by the lower grip weight) is sufficient to preclude proper aging. This interpretation is more consistent with the experimental observations; a sample aged in the TSAQ apparatus without the lower grip attached achieved S.D.C.'s of 33, 45, and 50% at 1,000, 5,000, and 10,000 psi respectively. Such an effect has been observed before, although not at such a low stress, in the Al-3Cu system as previously discussed.

G. FATIGUE

The test results are tabulated in Table II and plotted in Figure 29. For these specimens the endurance limit is approximately 29,000 to 30,000 psi. This agrees well with a previously determined [21] endurance limit of 29,000 to 36,000 psi for binary alloys. The manufacturer of this alloy has indicated an endurance limit for reversed bending of 19,000 psi [23]. Remembering that the specimens tested were in the as-heat treated condition, it would be expected that these test results are close to a low limit.

A cursory visual examination of the fracture surface revealed striking parallel fracture surface features (Figure 30). One specimen was sectioned longitudinally, perpendicular to the apparent plate surfaces. Microscopic examination disclosed the structure shown in Figure 31. Apparently the manufacturing and forming processes introduced inclusions. The result is a very definite, undesirable texture. The internal discontinuities, in some cases, appear to be the origin for small, curved cracks (Figure 31). These may also explain the presence of numerous small cracks on the fracture surface (Figure 32).

The specimens tested below 37,000 psi developed rather clean fracture surfaces perpendicular to the specimen axis. This was not the case for specimens tested above 37,000 psi. The later specimens exhibited a very rough, irregular fracture surface (Figure 30). At the higher stresses, fatigue cracks would develop along parallel planes and

finally link up by a shear failure along various discontinuities perpendicular to the plane of the fatigue crack. The resulting surface being highly irregular due to the internal structure.

Examination of the fracture surface with a SEM revealed the characteristic striations commonly associated with fatigue failures (Figure 33). The striations exist on many planes and seem to propagate in many directions (Figures 34, 35).

V. CONCLUSIONS

1. Incramute can be properly heat treated to produce significant damping capacity. The damping capacity measured at high stresses can easily exceed 35%.
2. The S.D.C. is extremely sensitive to aging time at a given temperature or temperature for a fixed time.
3. The effect of stress during heat treatment is significant. The experimental techniques used did not clearly separate the effect of stress during the aging process or during the quenching process although the stress effect appears to be on the aging process.
4. Tensile stress may slow down the $\gamma \rightarrow \omega$ reaction or speed up the $\gamma \rightarrow \alpha_{Mn}$ reaction.
5. There appears to be the ability to regain damping capacity after the apparent maximum has been passed.
6. An endurance limit of 29,000 psi can be expected for Intramute aged to its maximum damping condition (8 hours at 400°C).

VI. RECOMMENDATIONS

1. The stress dependence of the development of S.D.C. should be pursued more systematically, including determination of the effect of stress sign, stress level, and aging temperature in order to clearly delineate the affected process and mechanism.
2. M_s for "conditioned" alloys should be determined as a function of applied stress level during quenching.
3. The stress effects on the aging kinetics should be phenomenologically determined.
4. A more extensive investigation might warrant purchasing a B&K Complex Modulus Apparatus Type 3930 (Appendix A).
5. Optimal engineering methods for employing the material should be investigated. Because of their inherent damping capacity, powder metallurgy Mn-Cu alloys should be investigated.
6. The change in shear modulus during aging should be correlated with the damping capacity.

APPENDIX A
MEASUREMENT OF DAMPING CAPACITY

A survey of available literature indicated that there is no one generally accepted method of measuring damping capacity. The methods available can be grouped into seven categories:

1. decay of free vibration
2. resonant response
3. non-resonant forced vibration
4. wave-propagation methods
5. rotating beam deflection
6. composite oscillator
7. thermal methods

In some cases the particular method used was tailored to suit the damping mechanism involved.

Bert (30) covers the mathematical modeling involved in some of the more common experimental methods and develops the mathematical expressions to be used. Jensen (31) reported on several experimental techniques used by the Bureau of Mines. Among these was a torsional pendulum (32). The torsional pendulum had been recently used at NSRDC annapolis and was available for use.

It was decided to obtain the device for several reasons:

1. it was a proven device
2. it was available at no cost

3. it would provide data that could be easily compared to previously published work [2, 2, 9]

A strain gage mounted on the specimen provided the means of measuring the amplitude of successive vibrations of the specimen and inertia wheel. The specific damping capacity could be calculated from:

$$S.D.C. = \frac{A1^2 - A2^2}{A1^2} \quad 100$$

A. DAMPING CAPACITY MEASUREMENT: PULSE-ECHO (MHz) APPARATUS

It was considered desirable to also experimentally evaluate alternate techniques available to measure damping properties of high damping materials. Of particular interest was the measurement of damping properties at higher frequencies than available with the (very low frequency) torsion pendulum. As part of this effort, an ultrasonic pulse-echo apparatus was adapted and evaluated. This apparatus had been previously used in the NPS Physics Department of measure sould velocities and elastic constants in metallic single crystals. The equipment may also be used without modification to measure signal attenuation in polycrystalline alloys from which damping capacity can be directly calculated.

The specific apparatus provided for the generation and detection of pulses of ultrasonic specimen excitation of MHz frequencies. These pulses propagate from end to end in right circular specimens. A Matec generator/receiver was

used with a single quartz transducer bonded to one specimen end. This single transducer acted as both driver and pickup for echoed pulses. The reflected pulses were amplified and presented on an oscilloscope. Initially, .25 inch diameter, 1.0 inch long specimens were prepared with parallel polished ends and were driven using an x-cut piezoelectric crystal.

Attentuation (ultrasonic damping) was found to be so high in these materials that, using the indicated specimen geometry, echoes could not be detected at any pulse power level. For this reason, shorter specimens driven by larger transducers were prepared. Unfortunately these were no more successful than the earlier samples.

B. DAMPING CAPACITY MEASUREMENT: RESONANT BAR (KHz) METHOD

In addition to the techniques for damping capacity measurement mentioned above, several specimens (right circular cylinders 0.25 inches in diameter and 4.0 inches long) were prepared and taken to Los Alamos Scientific Laboratory, Los Alamos, New Mexico where Dr. P. Armstrong carried out measurements on an existing resonant bar device of the type normally used to determine Young's modulus. Results have been tabulated in Table III.

Damping properties obtained from the resonant bar technique are unfortunately not directly translatable to S.D.C. The general difficulty is that values obtained are unique to the particular experimental arrangement and specimen geometry so that only relative correlations can be made. In the

present case a reference sample of hard-drawn copper was used. "Incramute" and "Sonoston" samples (in the as-received condition) damped approximately six times as well as hard-drawn copper by this means of comparison.

An interesting observation can be made on the "Sonoston" resonant bar data which was obtained at two different vibration frequencies. It is notable that a decrease of 9 Hz driving frequency resulted in a tenfold increase in vibration amplitude. This relation is characteristic of a non-linear hardening spring (Figure 36) involving asymmetric resonance peaks (See Table A1 data). Because of the magnitude of the jump phenomena, it is believed that the non-linearity is not too great in this case.

C. DAMPING CAPACITY MEASUREMENT: COMPLEX MODULUS

B&K Instruments Inc. markets commercially a Complex Modulus Apparatus Type 3930 (Figure 37). This device magnetically excites strips of the sample material at one of its resonant frequencies. The device allows the material damping to be measured by three different methods:

1. vibration build-up rate
2. vibration decay rate
3. resonance quality factor

The apparatus is made of non-corrosive amagnetic metal. It is designed to operate over the temperature range from -150°C to 250°C making it possible to measure the properties of the material as a function of temperature also. The

frequency of the test is varied simply by varying the free length of the clamped bar and employing the different resonance modes.

The main reason for not pursuing the acquisition of an apparatus was cost. The apparatus alone costs $1500. The electronics necessary for the system are even more expensive.

Also to be considered was the effect of high damping on the determination of the resonance quality factor. The higher the damping the flatter would be the resonance curve thus increasing the difficulty and uncertainty in obtaining a value for the resonance quality factor.

If an on-going, detailed investigation were to be conducted, such a device should be seriously considered. The simple geometry required and the temperature capability of the device would be a great advantage.

D. DAMPING CAPACITY MEASUREMENT: RESONANT DWELL DAMPING APPARATUS

In the preliminary investigations of the damping capacity of "Incramute" [20], a resonant dwell damping apparatus constructed by Bold Beranek and Newman was used (Figure 38). The flat specimen is mounted as a cantilever and excited in the fundamental mode by a shaker. The energy dissipated is determined from the resonant amplification factor. The deflection of the beam is measured with a calibrated lens in a monocular microscope. Utilizing the stress-strain relationship for a cantilever beam allows the deflection to be converted to stress amplitude.

However, "unfortunately the resonant magnification factor is dependent upon the structural system configuration as well as upon the damping property of the material, so that it is considered to be a system characteristic rather than a basic material property."[1]

---

[1]Bert, C. W., Journal of Sound and Vibration, vol 29, p 136, 1973

APPENDIX B
UNCERTAINTY ANALYSIS

The uncertainty analysis was done in accordance with the method set forth by Kline and McClintock (33).

A. UNCERTAINTY IN CALCULATIONS OF S.D.C.

The equation for S.D.C. is:

$$S.D.C. = \frac{A1^2 - A2^2}{A1^2} \quad 100$$

so the uncertainty is

$$\omega_S = \left[\left(\frac{\partial S.D.C.}{\partial A1}\omega_A\right)^2 + \left(\frac{\partial S.D.C.}{\partial A2}\omega_B\right)^2\right]^{1/2}$$

where

$$\frac{\partial S.D.C.}{\partial A1} = \left[\frac{1}{A1} - \frac{2(A1^2 - A2^2)}{A1^3}\right]100$$

$$\frac{\partial S.D.C.}{\partial A2} = -\frac{2A2}{A1^2}\,100$$

finally

$$\omega_S = \left\{\left[\left(\frac{1}{A1} - \frac{2(A1^2-A2^2)}{A1^3}\right)100\,\omega_A\right]^2 + \left[\frac{2A2}{A1}\,100\,\omega_B\right]^2\right\}^{1/2}$$

The values for ω_A and ω_B were estimated to be:

$$\omega_A = \omega_B = 0.2$$

A computer program was used to compute S.D.C. and . Tables IV, V, VI, and VII present the results for the aging investigations of time and temperature dependence, Tables VIII, IX, and X present the results for the compression tests.

B. UNCERTAINTY IN STRAIN GAGE CALIBRATION

The shear stress on the surface of a specimen with a circular cross section is computed from:

$$S_s = \frac{Tc}{J}$$

where

$$J = \frac{\pi d^4}{32}$$

and because of the string-weight calibration system,

$$T = \frac{W D}{2}$$

The uncertainty in the shear stress is computed from:

$$\omega_{ss} = \left[\left(\frac{C}{J}\omega_T\right)^2 + \left(\frac{T}{J}\omega_c\right)^2 + \left(\frac{TC}{J^2}\omega_J\right)^2\right]^{1/2}$$

where

$$\omega_J = \frac{\pi d^3}{8}$$

$$\omega_T = \left[\left(\frac{d}{2}\omega_w\right)^2 + \left(\frac{W}{2}\omega_d\right)^2\right]^{1/2}$$

The following values were the estimations used for the calculations:

$$\omega_d = .001 \text{ inch}$$

$$\omega_w = .01 \text{ lb.}$$

$$\omega_c = .0005 \text{ inch}$$

the results are tabulated in Table XI.

C. UNCERTAINTY IN FATIGUE STRESS CALCULATIONS

The stress on a specimen in the R. R. Moore fatigue machine is calculated from:

$$S = \frac{2 F l}{\pi r^3}$$

and the uncertainty is calculated from:

$$\omega_{RR} = \left[\left(\frac{2F}{\pi r^3}\omega_l\right)^2 + \left(\frac{2l}{\pi r^3}\omega_w\right)^2 + \left(\frac{6Fl}{\pi r^4}\omega_r\right)^2\right]^{1/2}$$

which can be simplified to:

$$\omega_{RR} = \left[(.1794F)^2 + (.8049) + (9.184F)^2\right]^{1/2}$$

where the following estimates were used:

l = 5 inches

r = .151 inches

ω_r = .0005 inches

ω_l = .001 inches

ω_w = .01 pounds

The results are tabulated in Table XII.

APPENDIX C

TABLE I

Results of Tensile Stress Tests
Conducted at 400°C

Level of Stress (%Y.S.)		Aging Time (HRS)	S.D.C. (%)
Age	Quench		
.09	.09	4	0-2
.09	.09	6	0-2
.09	.09	8	0-2
.09	.09	10	0-2
.09	.09	12	0-2
1.0	1.0	8	0-2
4.94	.09	0.5	0-2
4.94	.09	1	0-2
4.94	.09	1.5	0-2
4.94	.09	2	0-2
4.94	.09	3	0-2
4.94	.09	4	0-2
4.94	.09	6	0-2
4.94	.09	8	0-2
.09	4.94	8	0-2
20	20	0.25	0-2
20	20	0.5	0-2
20	20	0.5	0-2

Level of Stress (%Y.S.)		Aging Time (HRS)	S.D.C. (%)
Age	Quench		
20	20	0.75	0-2
20	20	1	0-2
20	20	1	0-2
20	20	1.5	0-2
20	20	1.5	0-2
20	20	2	2.1
20	20	6	0-2
20	20	8	0-2
20	20	12	0-2
20	20	16	0-2
20	20	22	0-2
20	20	26	0-2
20	20	30	0-2
20	.09	6	0-2
.09	20	8	0-2
40	40	0.5	0-2
40	40	1	0-2
40	40	1.5	0-2
40	40	2	0-2
60	60	0.5	0-2

TABLE II

Results of Testing Incramute Specimens (Aged 8 hours at 400°C) in a R.R. Moore High Speed Fatigue Machine

Maximum Stress (psi)	Cycles to Failure
26,430	4.38×10^7 (no failure)
28,190	5.74×10^7 (no failure)
30,835	1.495×10^6
35,240	1.066×10^6
37,000	3.08×10^5
39,645	1.73×10^5
44,050	1.24×10^5
48,455	6.2×10^4
52,860	3.7×10^4

Material	ℓ in	$\bar{d}$ in	W g.	ρ g/cc	f_ℓ Hz	$f_{\frac{1}{2}}+$	$f_{\frac{1}{2}}-$	E 10^6psi	tan α 10^{-3}
Incramute (longitudinal)	4.114	0.240	22.726	7.451	16806	16937	16716	13.333	7.59
Incramute (transverse)	3.919	0.239	21.422	7.435	17716	17862	17626	13.416	7.69
Nitinol	4.043	0.2505	21.1586	6.480	16896	16948	16874	11.319	2.53
Sonoston	4.0105	0.2515	23.186	7.102	16701	16830	16619	11.926	7.29
Sonoston*	"	"	"		16692	16794	16597	11.913	6.81
Copper hard drawn	4.503	0.2495	30.0920	8.341	16653	16674	16633	17.557	1.42

* Amplitude of vibration ten times previous measurement

$E = 3.7432 \times 10^{-4} f^2 \ell^2 \rho$ where

f= resonant frequency, Hz

ℓ= length, inches

ρ= density, g/cc.

$\tan \alpha$ = internal friction = $\frac{L_f}{\sqrt{3}\, f}$ where Δf = freq. difference at half amplitude

1 Measurements made by P. E. Armstrong at Los Alamos Scientific Laboratory.

TABLE III

Table of Resonant Bar Damping Values[1]

TABLE IV

Uncertainty in S.D.C. for Specimens Aged at 350°C

Time	Surface Shear Stress 1000 psi	5000 psi	10000 psi
4 Hrs.	2.4±1.7	1.5±1.7	1.5±1.7
8 Hrs.	0.7±1.8	0.8±1.9	3.1±1.7
12 Hrs.	1.6±1.8	1.7±1.9	2.4±1.8
16 Hrs.	1.6±1.9	1.5±1.7	1.4±1.7
20 Hrs.	0.7±1.8	0.7±1.8	1.5±1.7
24 Hrs.	0.7±1.8	1.5±1.8	2.9±1.7
26 Hrs.	3.7±1.7	3.4±1.9	6.8±1.6
28 Hrs.	6.9±1.6	3.2±1.7	6.3±1.8
30 Hrs.	22.2±1.4	12.5±1.5	6.7±1.6
32 Hrs.	32.1±1.3	19.6±1.4	15.5±1.5
34 Hrs.	30.5±1.4	21.1±1.4	19.1±1.4
36 Hrs.	29.1±1.2	24.9±1.5	23.4±1.4
38 Hrs.	36.1±1.4	28.2±1.3	25.2±1.3
42 Hrs.	24.1±1.5	36.5±1.3	28.0±1.4
46 Hrs.	34.5±1.2	41.4±1.2	36.1±1.2
50 Hrs.	24.2±1.5	39.4±1.2	40.4±1.1

TABLE V

Uncertainty in S.D.C. for Specimens Aged at 400°C

Time	Surface Shear Stress 1000 psi	5000 psi	10000 psi
2 Hrs.	5.6±1.7	2.5±1.8	8.6±1.9
6 Hrs.	15.5±1.6	12.7±1.9	(1)
6 Hrs.	27.0±1.4	31.6±1.4	30.1±1.6
8 Hrs.	36.0±1.4	40.4±1.5	37.3±1.4
10 Hrs.	10.2±1.8	35.6±1.2	40.2±1.5

TABLE VI

Uncertainty in S.D.C. for Specimens Aged at 450°C

Time	Surface Shear Stress 1000 psi	5000 psi	10000 psi
.5 Hrs.	2.4±1.8	3.8±1.7	7.8±1.7
1. Hrs.	10.5±1.9	11.7±1.7	10.4±1.6
1.5 Hrs.	19.4±1.5	22.9±1.5	24.3±1.6
2.0 Hrs.	25.0±1.7	25.1±1.4	26.9±1.5
2.5 Hrs.	12.6±1.7	24.4±1.4	26.5±1.5

[1]Unable to twist specimen enough to obtain this reading

TABLE VII

Uncertainty in S.D.C. for Specimens Aged at 500°C

Time	Surface Shear Stress 1000 psi	5000 psi	10000 psi
0.5 Hrs.	6.6±2.4	7.8±1.9	9.6±1.6
1.0 Hrs.	7.1±3.0	6.8±2.1	13.7±1.9
1.5 Hrs.	5.5±1.6	6.5±1.6	11.2±1.5

TABLE VIII

Uncertainty in S.D.C. for Specimens Aged at 400°C Loaded to 2.85% Y.S. in Compression During Age and Quench

Time	Surface Shear Stress 1000 psi	5000 psi	10000 psi
2 Hrs.	0.7±1.8	0.6±1.5	4.7±1.5
4 Hrs.	0.7±1.6	1.3±1.6	2.1±1.5
6 Hrs.	28.7±1.3	19.7±1.3	18.3±1.4
8 Hrs.	31.7±1.2	25.8±1.2	25.4±1.2
10 Hrs.	21.5±1.3	33.9±1.3	30.2±1.3
11 Hrs.	34.9±1.3	36.0±1.2	32.6±1.2
13 Hrs.	21.6±1.4	35.6±1.2	37.8±1.2

TABLE IX

Uncertainty in the S.D.C. for Specimens Aged at 400°C Loaded to 2.85% Y.S. in Compression During Age Only

Time	Surface Shear Stress 1000 psi	5000 psi	10000 psi
2 Hrs.	0.7±1.8	1.4±1.7	4.6±1.7
4 Hrs.	7.1±1.7	7.6±1.6	14.2±1.5
6 Hrs.	25.9±1.4	21.2±1.5	17.3±1.5
8 Hrs.	25.0±1.4	29.4±1.3	28.0±1.3
10 Hrs.	19.3±1.4	36.5±1.2	43.3±1.1
12 Hrs.	26.6±1.3	38.2±1.2	42.9±1.2
14 Hrs.	19.8±1.4	37.8±1.2	39.2±1.2

TABLE X

Uncertainty in the S.D.C. for Specimens Aged at 400°C Loaded to 2.85% Y.S. in Compression During Quench Only

Time	Surface Shear Stress 1000 psi	5000 psi	10000 psi
2 Hrs.	0.7±1.8	5.7±1.5	7.0±1.5
4 Hrs.	3.8±1.7	7.6±1.6	11.6±1.5
6 Hrs.	24.4±1.3	26.7±1.4	18.5±1.5
8 Hrs.	35.3±1.3	31.4±1.4	20.1±1.6
10 Hrs.	27.4±1.4	37.8±1.2	34.5±1.2
12 Hrs.	14.7±1.5	38.7±1.3	37.5±1.2
14 Hrs.	9.3±1.3	34.0±1.2	42.2±1.2

TABLE XI

Uncertainty in Surface Shear Stress

Surface Shear Stress		
1000 psi	5000 psi	10000 psi
±20 psi	±103 psi	±205 psi

TABLE XII

Uncertainty in Fatigue Stress

Stress (psi)	Uncertainty (psi)
26430	± 277
28190	± 306
30835	± 334
35240	± 382
37000	± 401
39645	± 430
44050	± 478
48455	± 526
52860	± 574

APPENDIX D

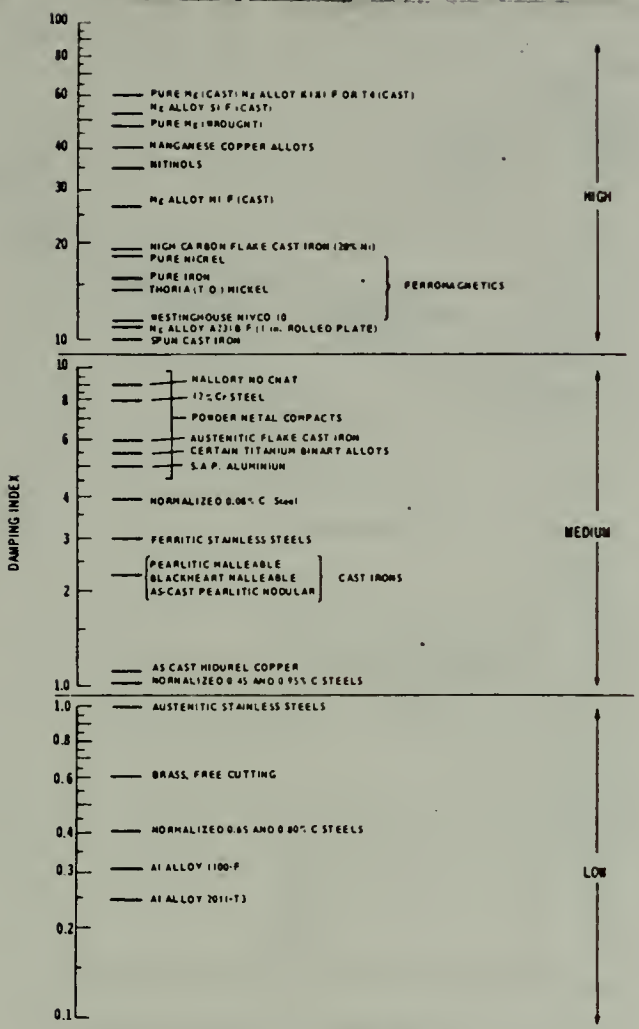

Less than 0.2 Mg alloys AZ91C-T4 (cast) AZ81XA-T4 (cast) Al alloys 2017-T4; Allegheny Ludlum alloys hi-temp 25, N-155, 19-9DL, S-816. Most commercial titanium alloys. Brasses and bronzes. Many ferrous and non-ferrous alloys not listed above.

FIGURE 1. Damping Index Data (from Jones (34))

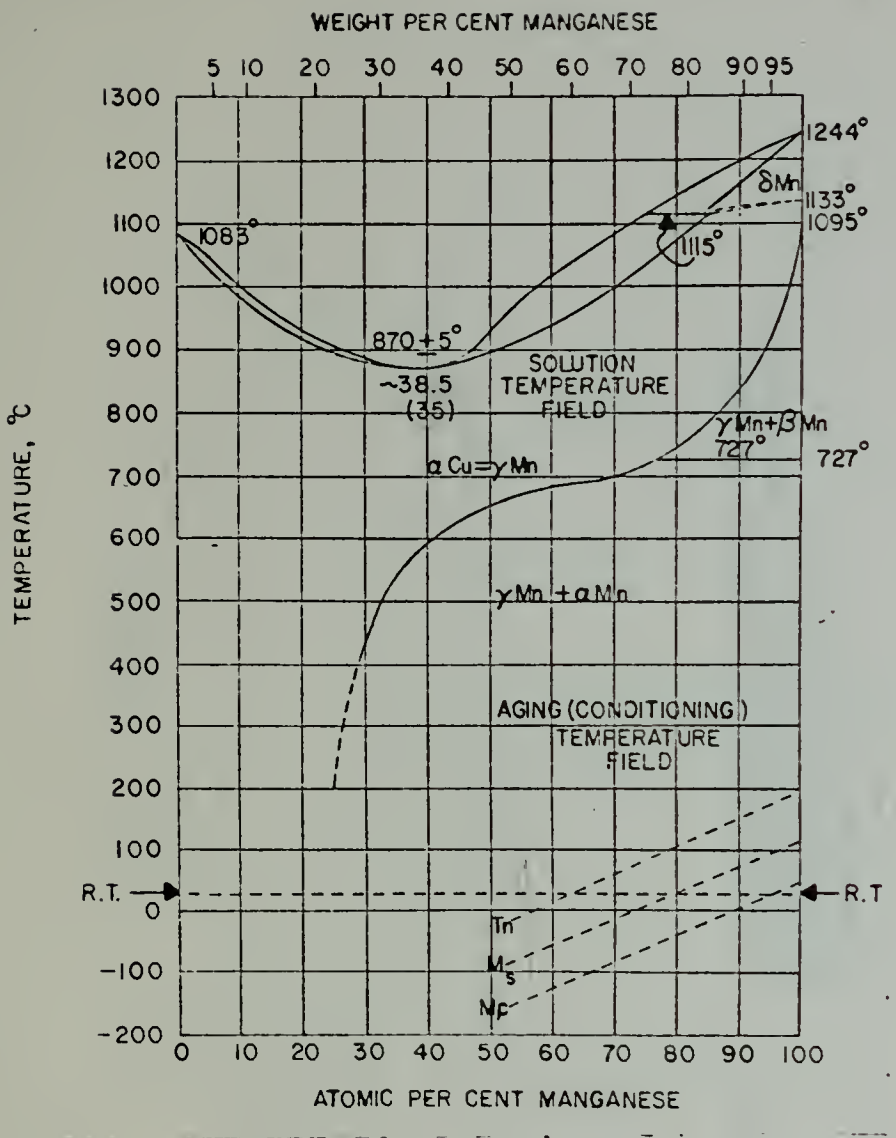

FIGURE 2. Mn-Cu Equilibrium Phase Diagram and Approximate T_N, M_s, and M_f Metastable Phase Transition Temperatures (from Perkins (26))

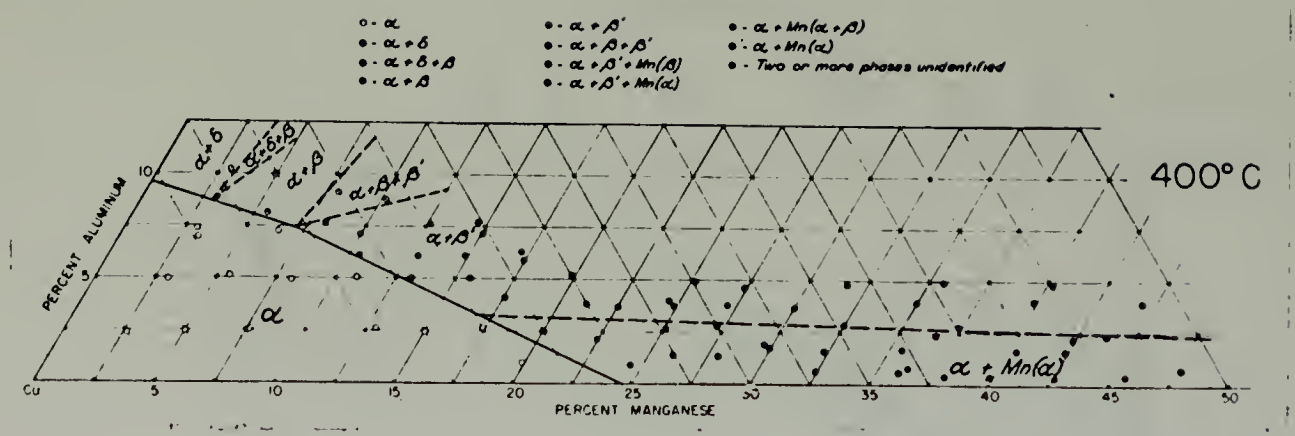

FIGURE 3. Copper-Manganese-Aluminum System, the Phase Boundaries of the Copper-Rich Corner at 400°C (from Dean (17))

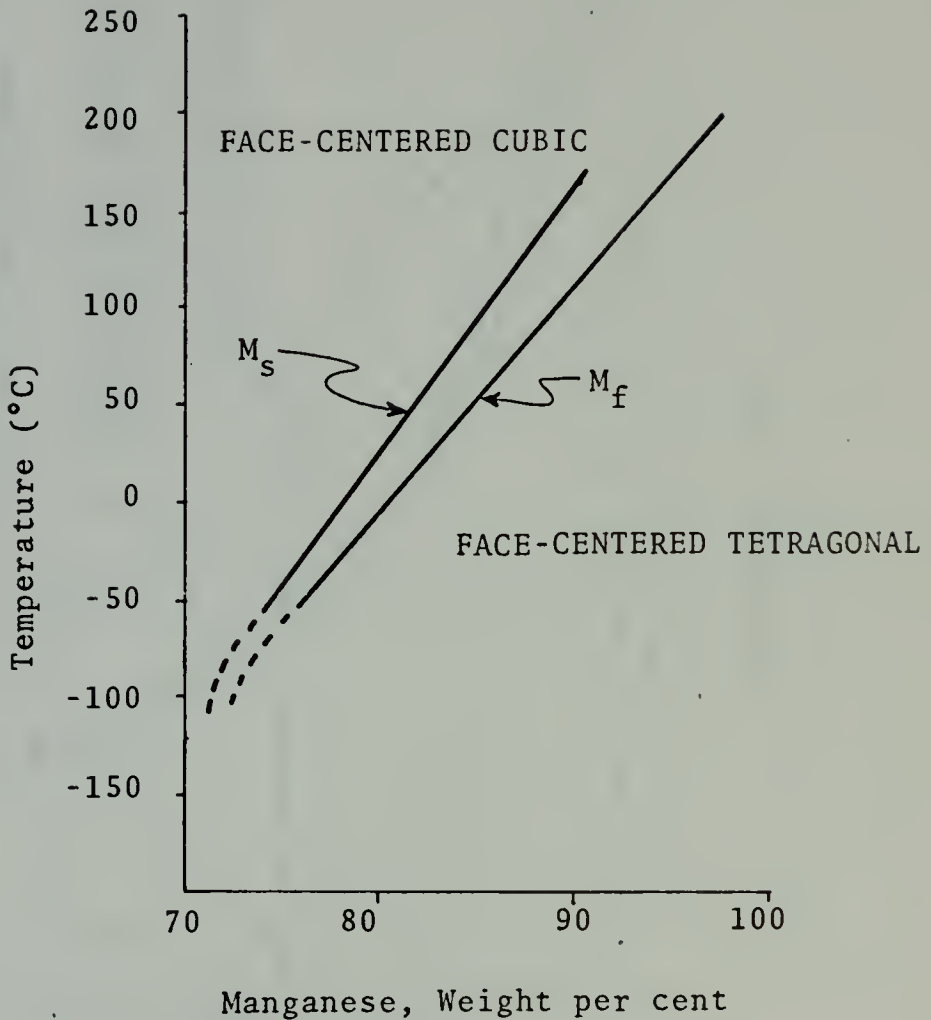

FIGURE 4. M_s, M_f Curves as a Function of Temperature and Composition (from Basinski and Christian (35))

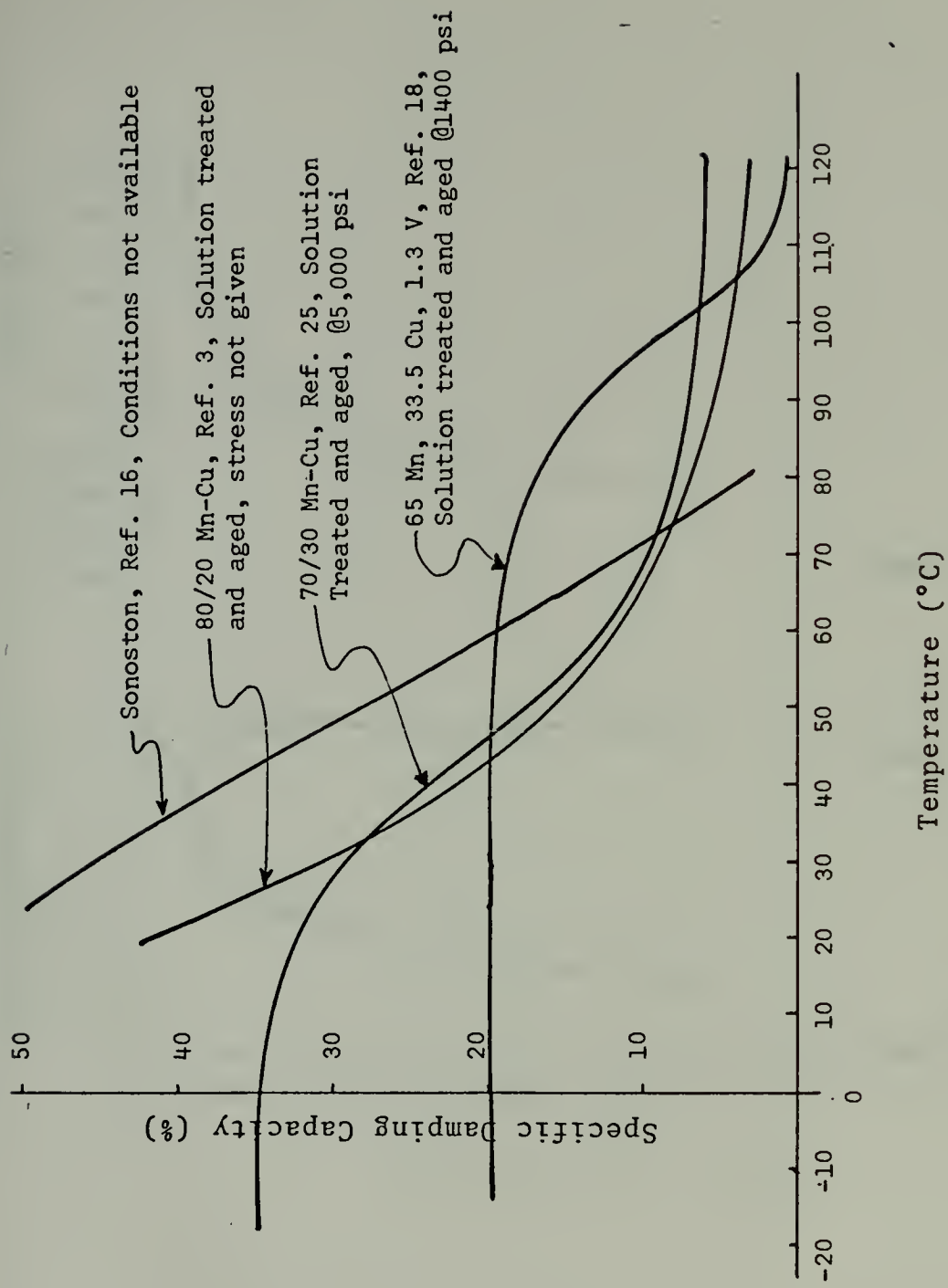

FIGURE 5. Effect of Temperature on the Damping Capacity of Mn-Cu Alloys

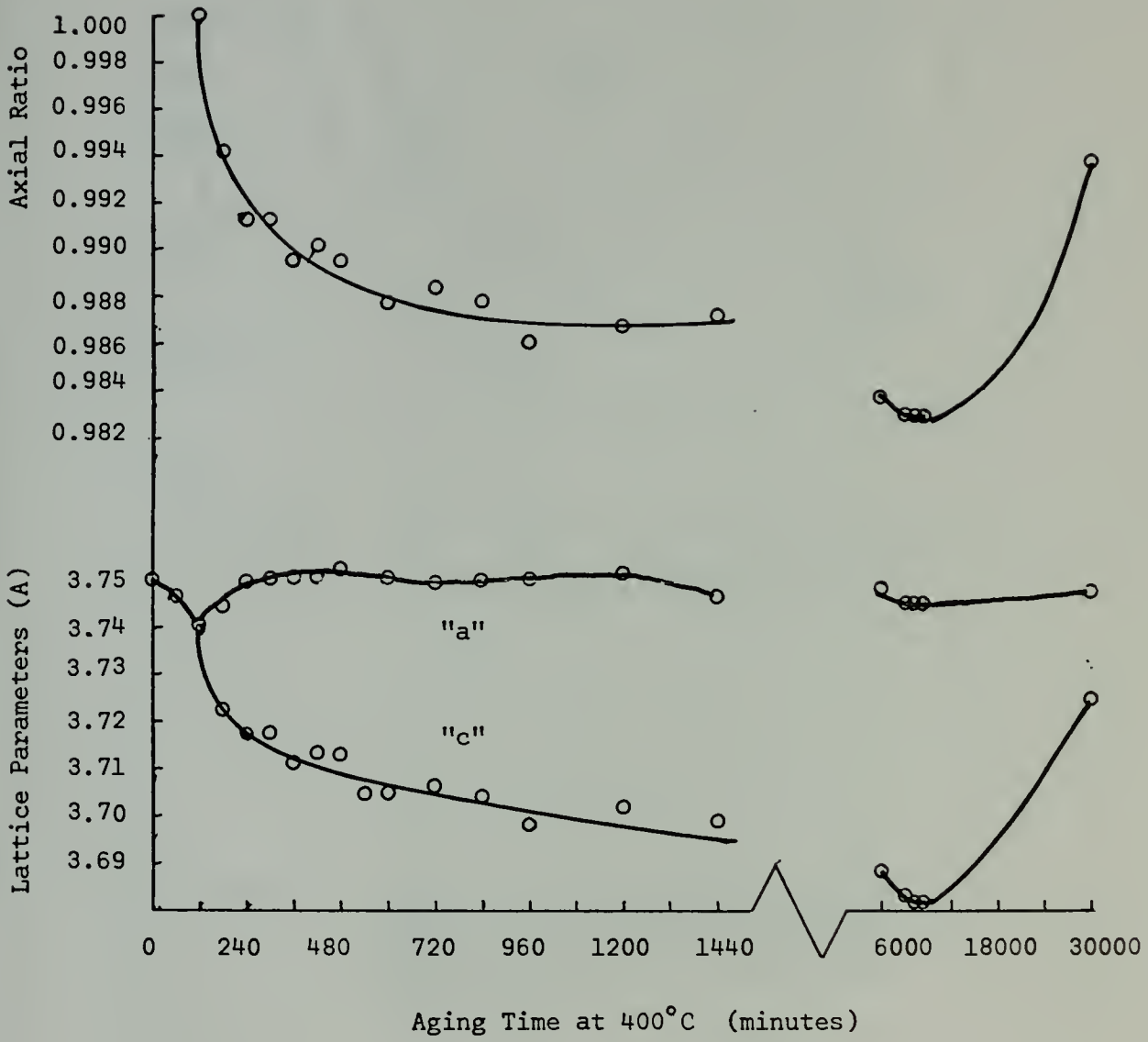

FIGURE 6. Change in Lattice Parameters and Axial Ratio in a 57% Mn Alloy Aged for Various Times at 400°C (from Hedley (13))

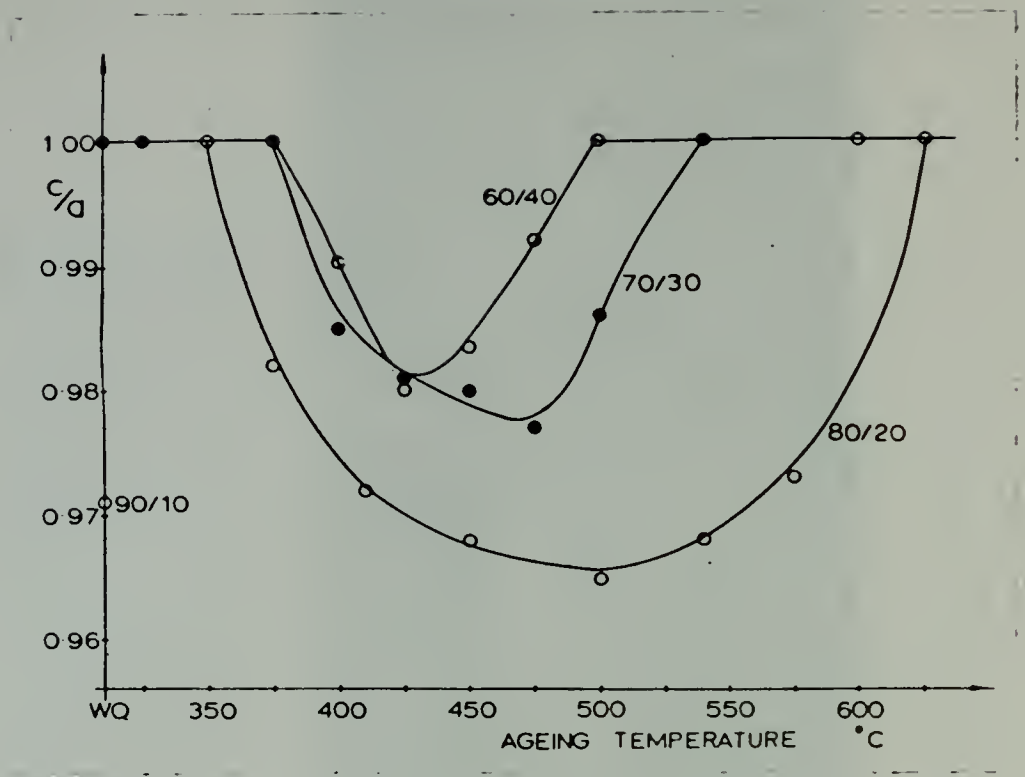

FIGURE 7. Variation in c/a Ratio for 60/40, 70/30, and 80/20 Mn-Cu Alloys Aged for 2 Hours at Different Temperatures (from Butler and Kelley (15))

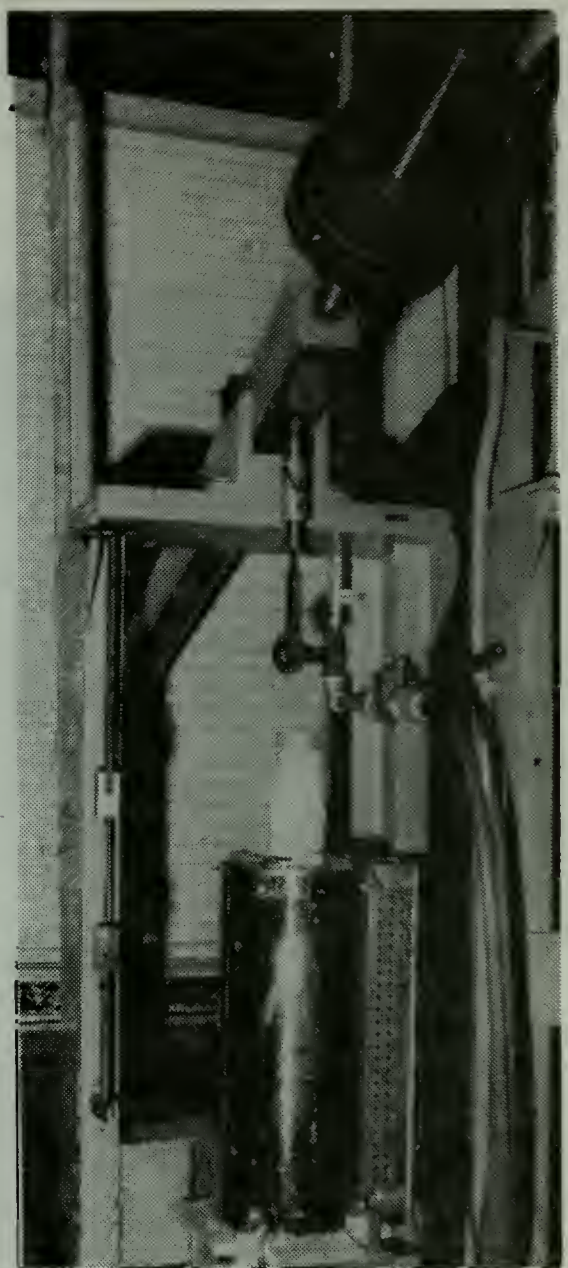

FIGURE 8. Tension Stress-Age-Quench Apparatus and Furnace

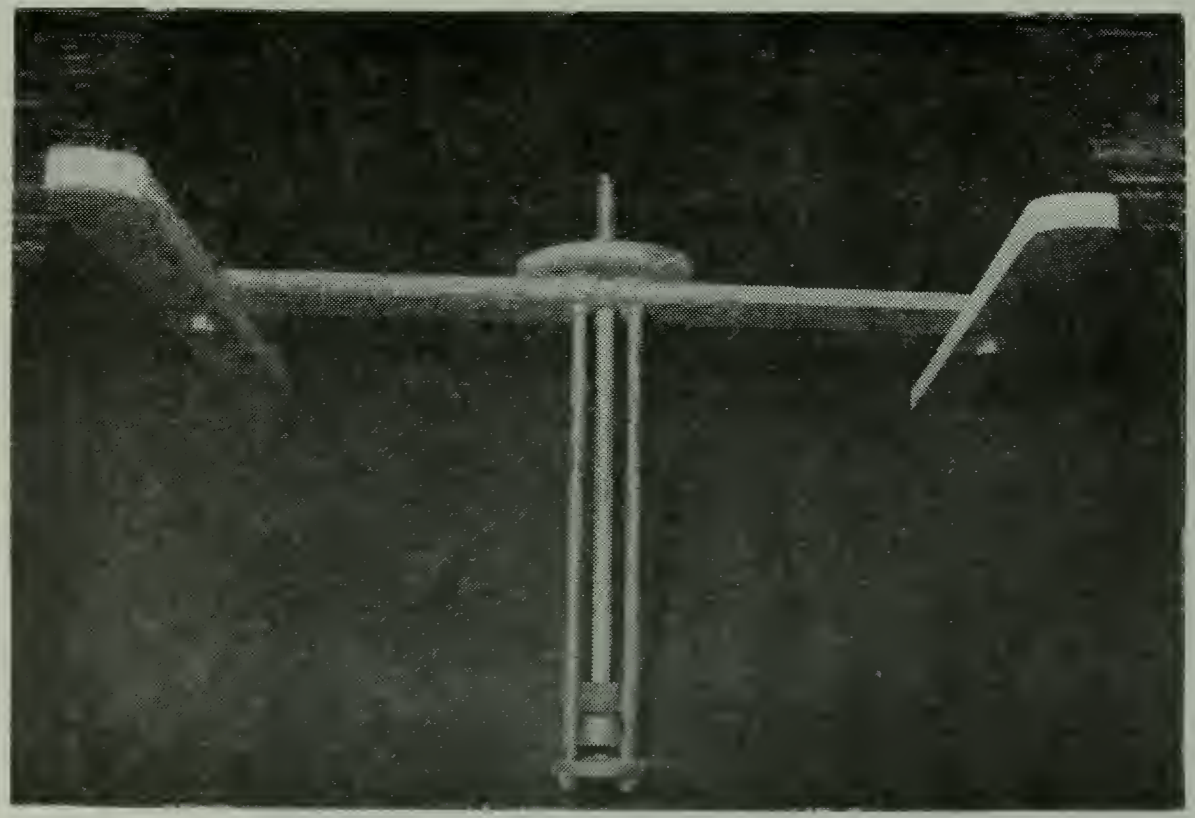

FIGURE 9. Compression Stress-Age-Quench Apparatus

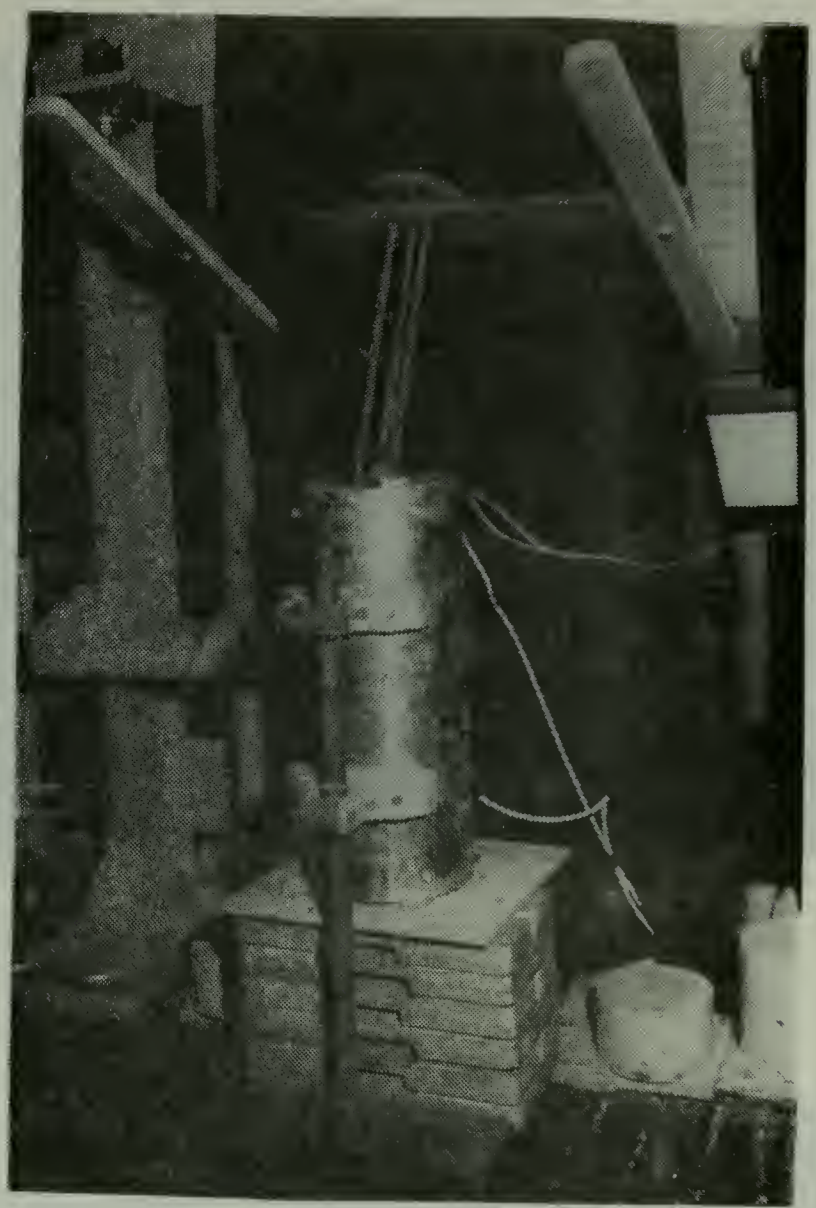

FIGURE 10. Compression Stress-Age-Quench Apparatus and Furnace

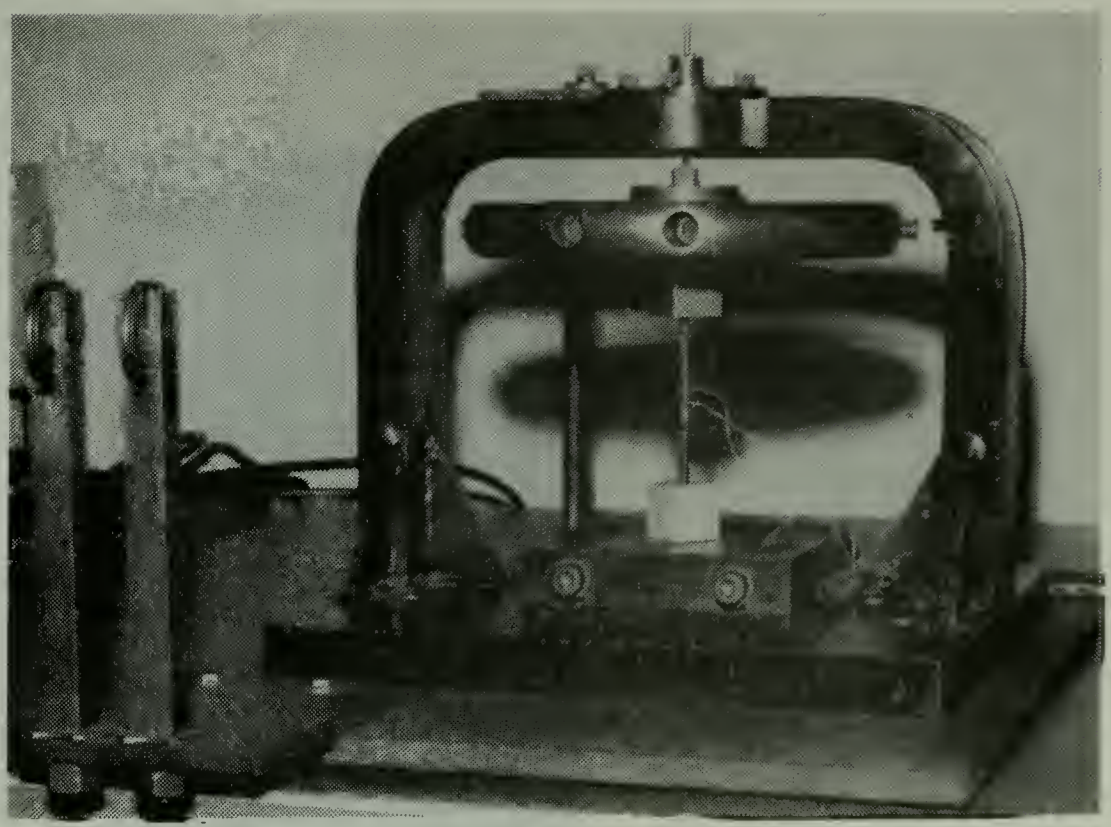

FIGURE 11. Torsion Pendulum and Specimen Arrangement

FIGURE 12. Specimen Used in Tension and Compression Stress-Age-Quench Apparatus

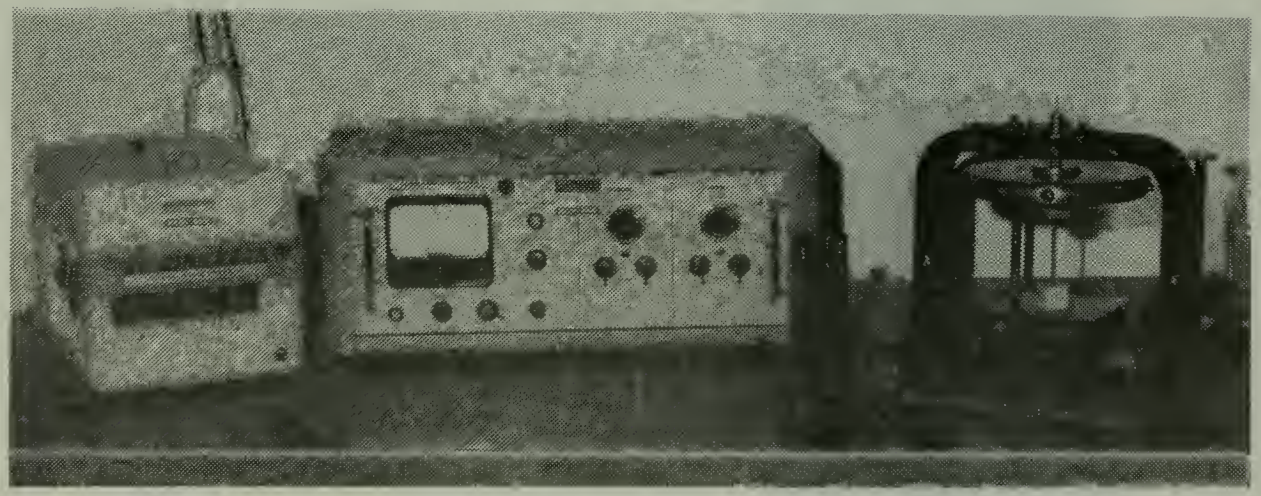

FIGURE 13. Torsion Pendulum Apparatus

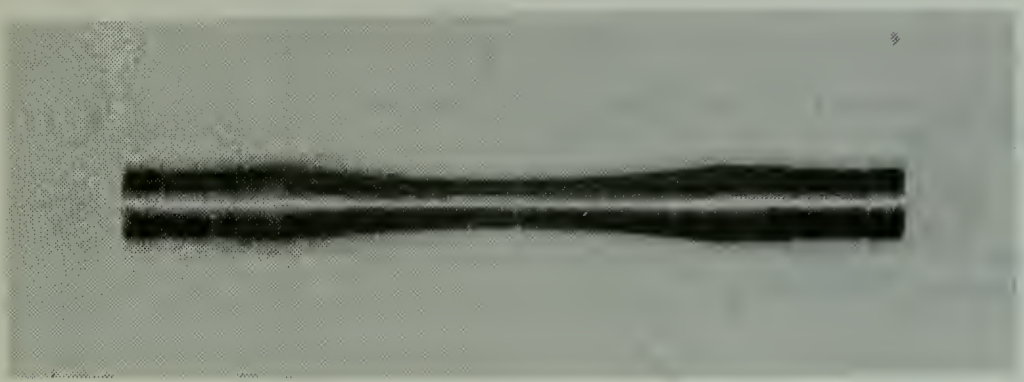

FIGURE 14. Fatigue Specimen Geometry

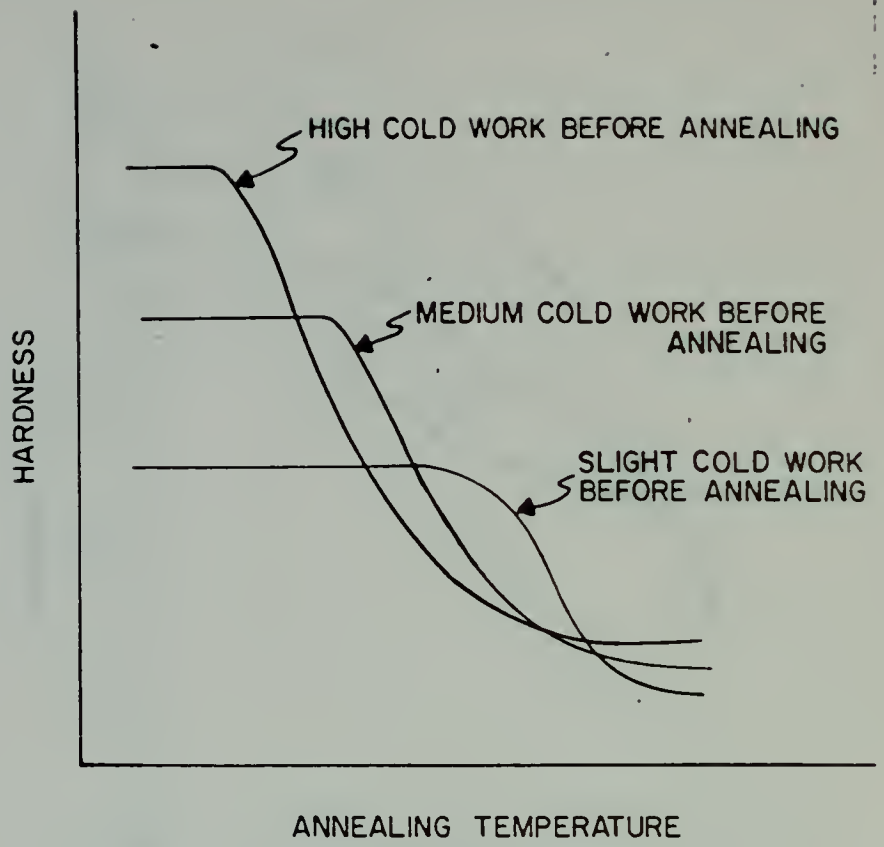

FIGURE 15. Typical Recrystallization Annealing Curves

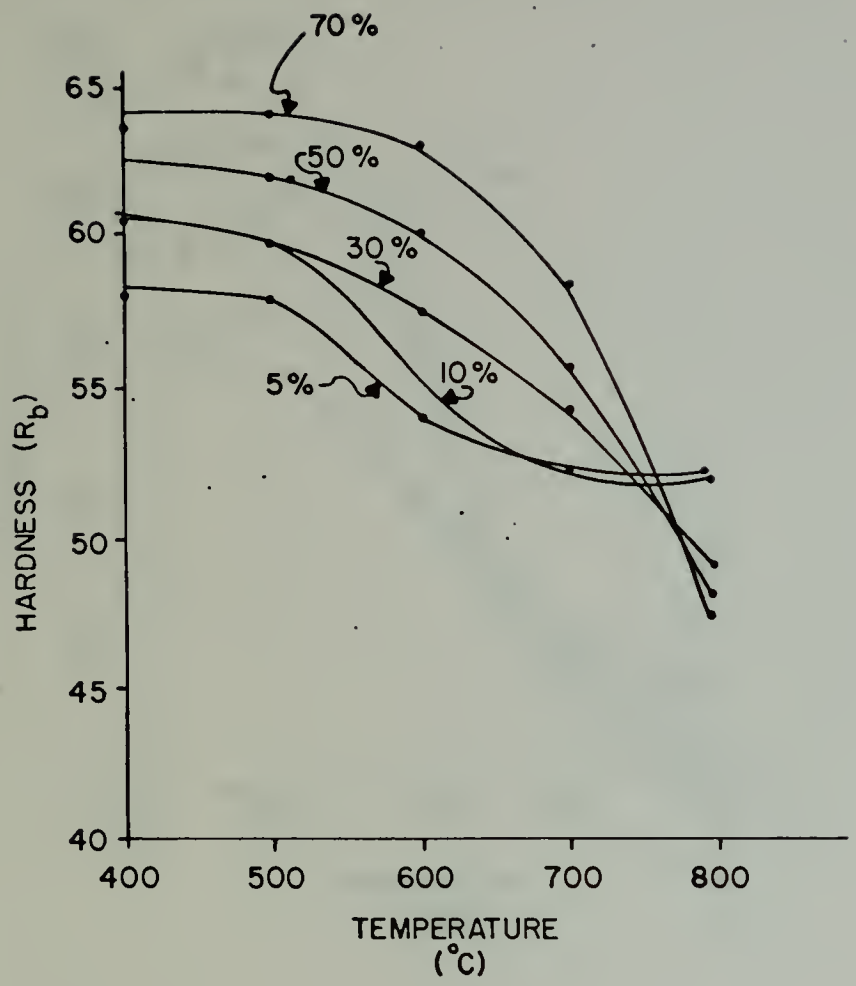

FIGURE 16. Experimental Annealing Curves for "Sonoston" for Various Amounts of Cold Work

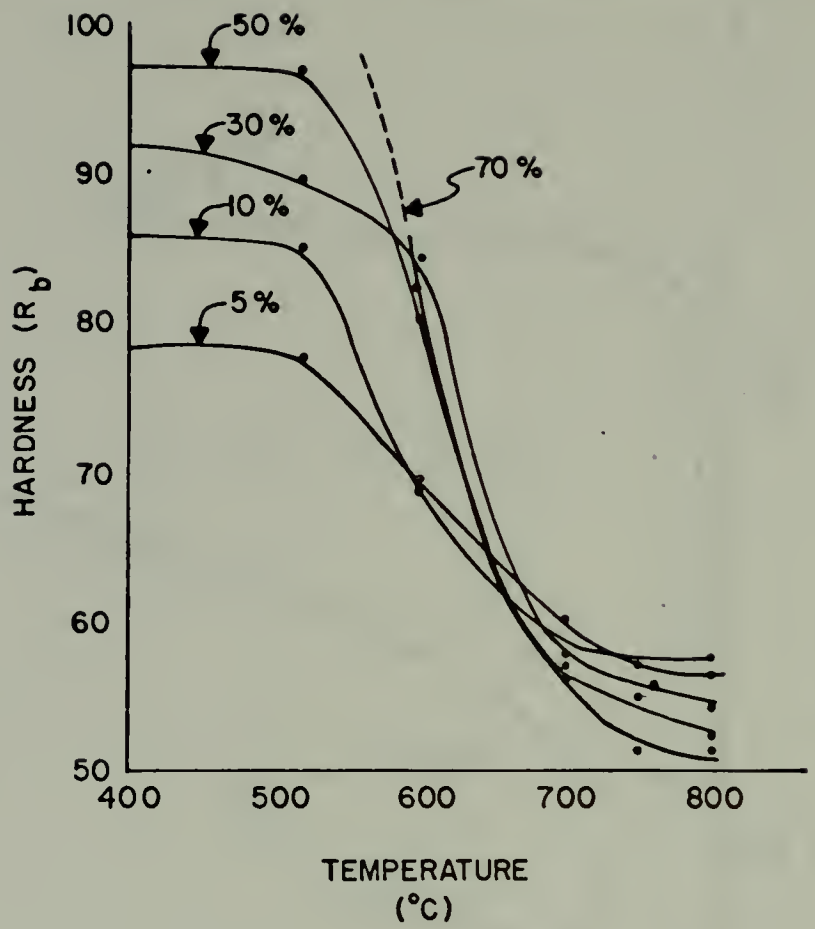

FIGURE 17. Experimental Annealing Curves for "Incramute" for Various Amounts of Cold Work

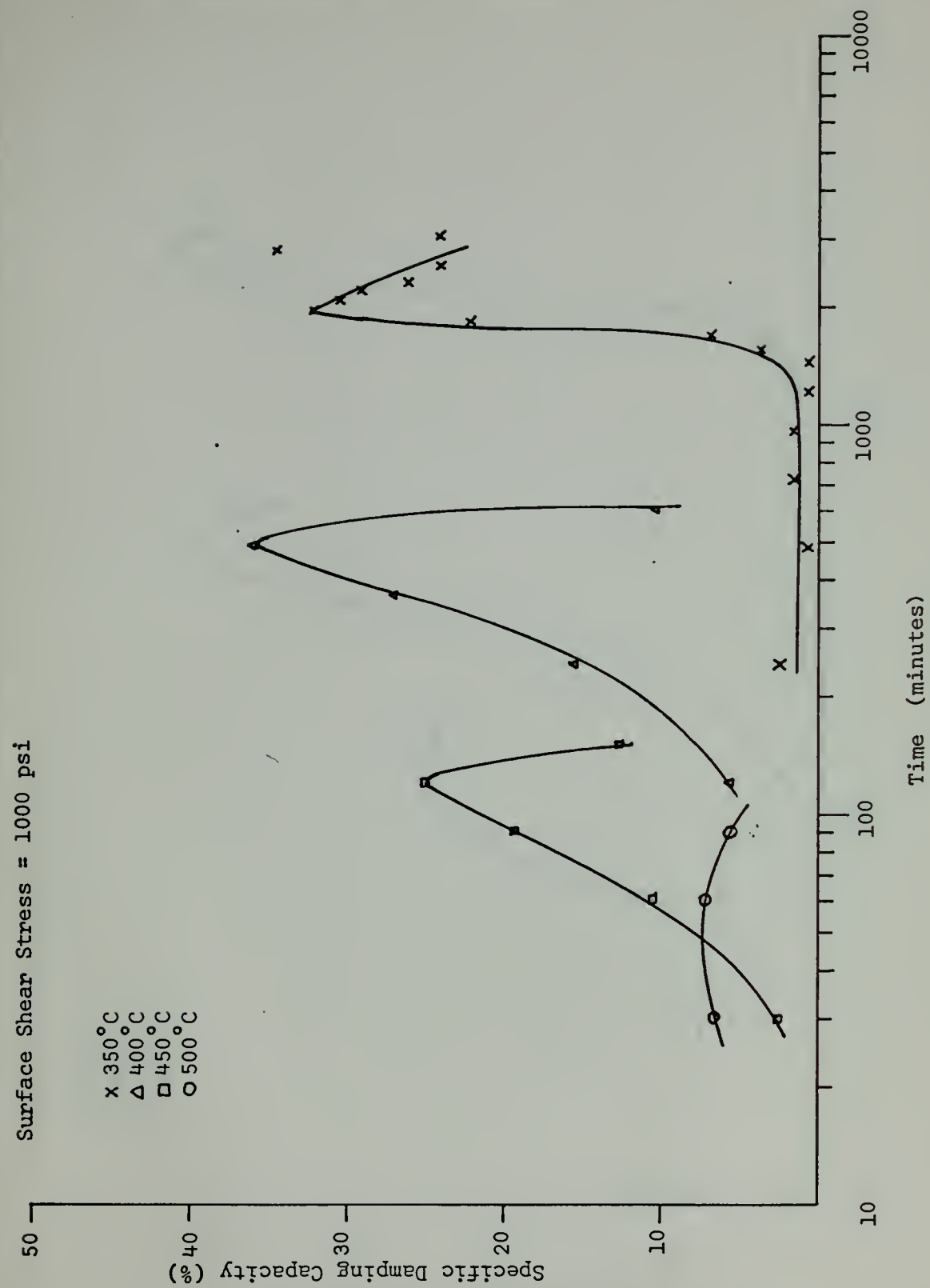

FIGURE 18. Effect of Aging Time on Damping Capacity When Measured at 1000 psi Surface Shear Stress

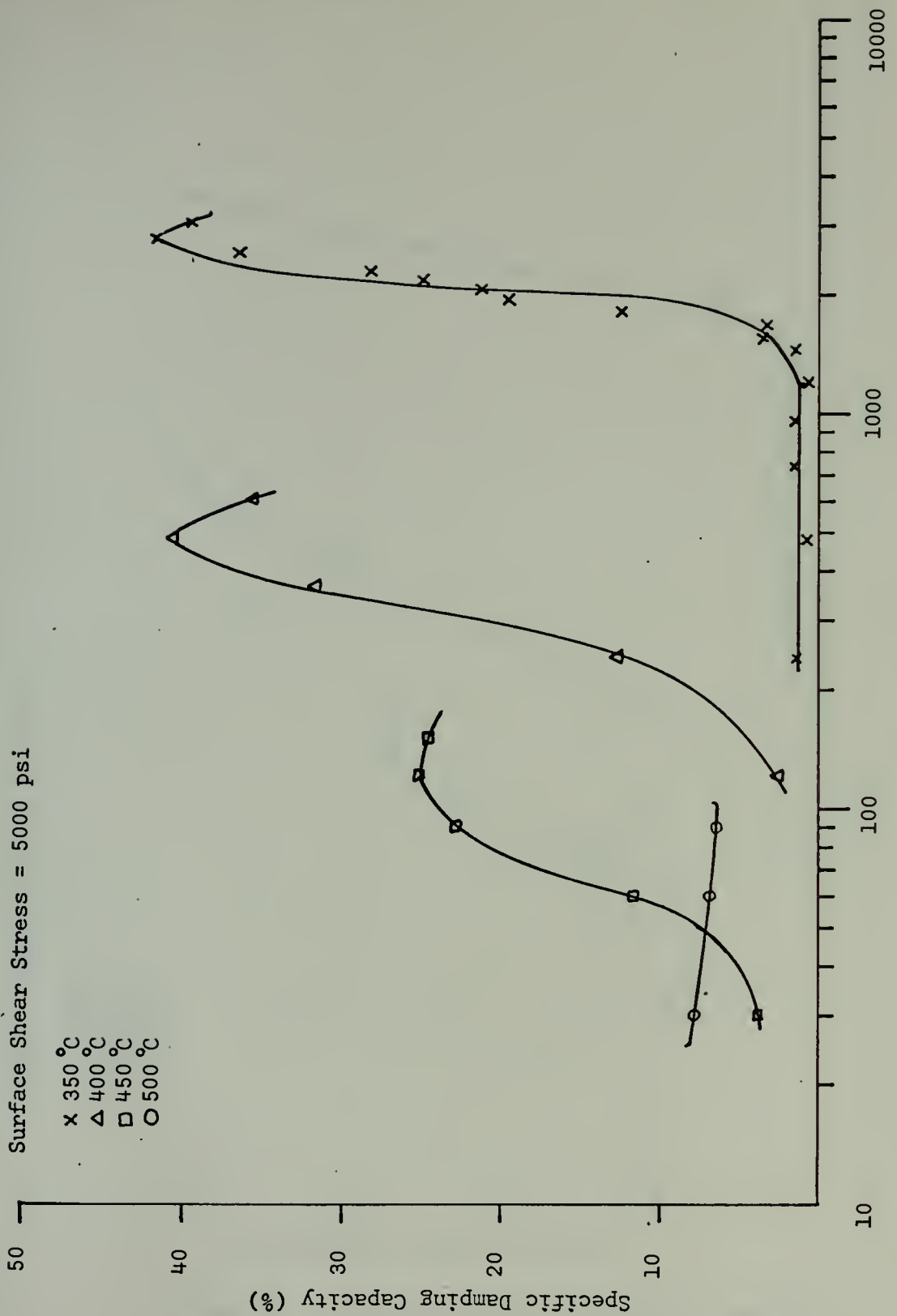

FIGURE 19. Effect of Aging Time on Damping Capacity When Measured at 5000 psi Surface Shear Stress

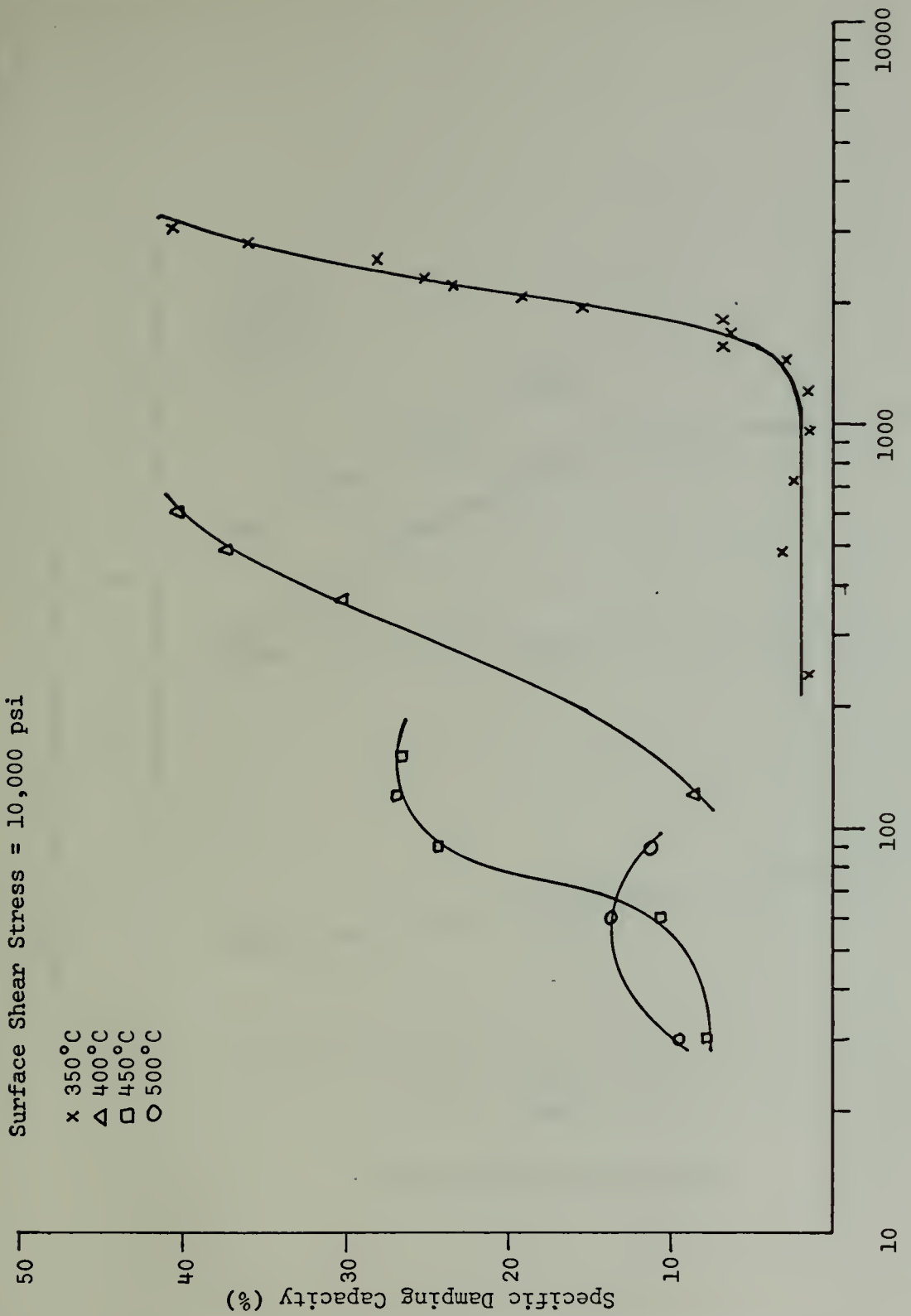

FIGURE 20. Effect of Aging Time on Damping Capacity When Measured at 10000 psi Surface Shear Stress

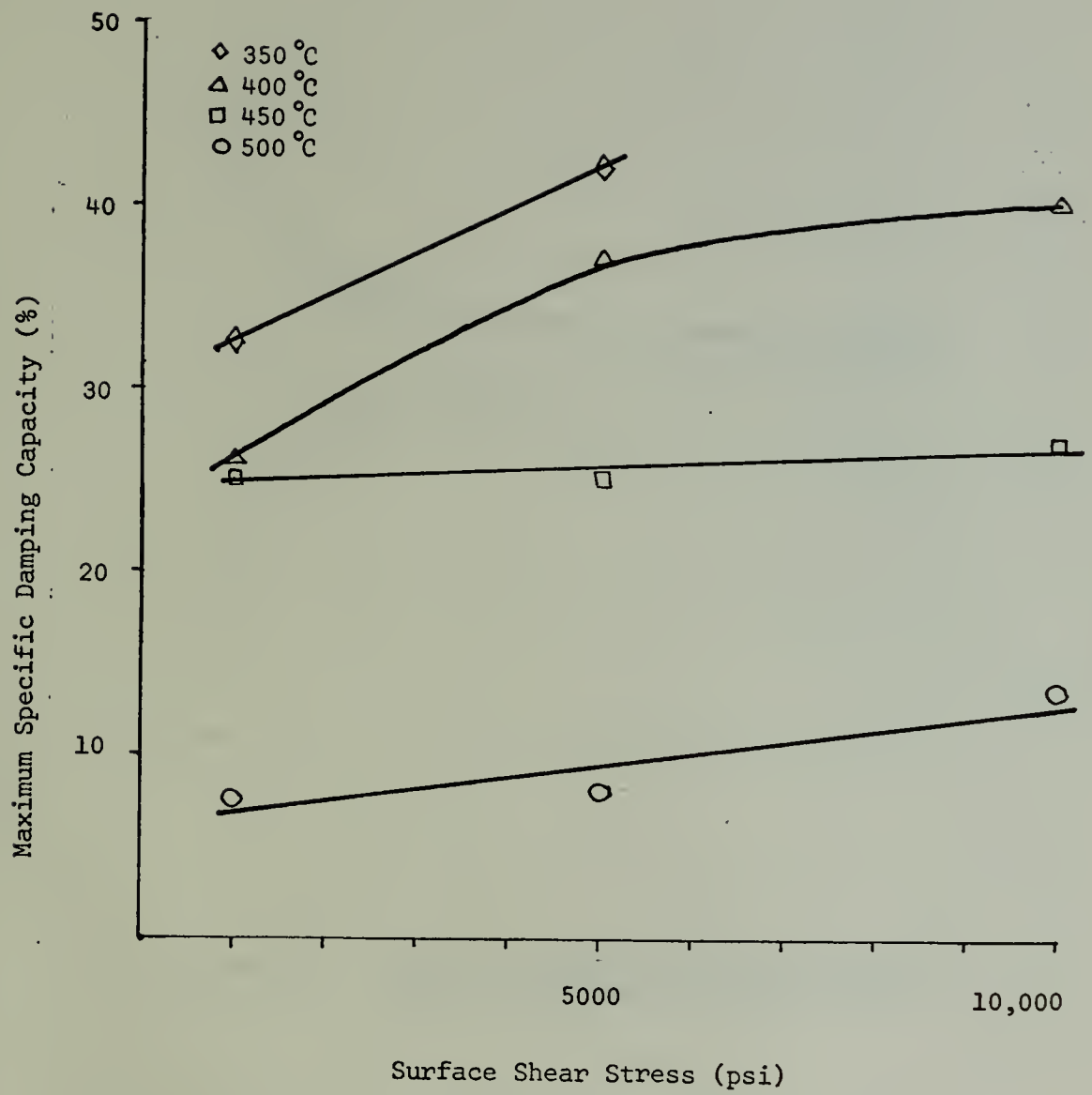

FIGURE 21. Effect of Aging Temperature on Maximum S.D.C.

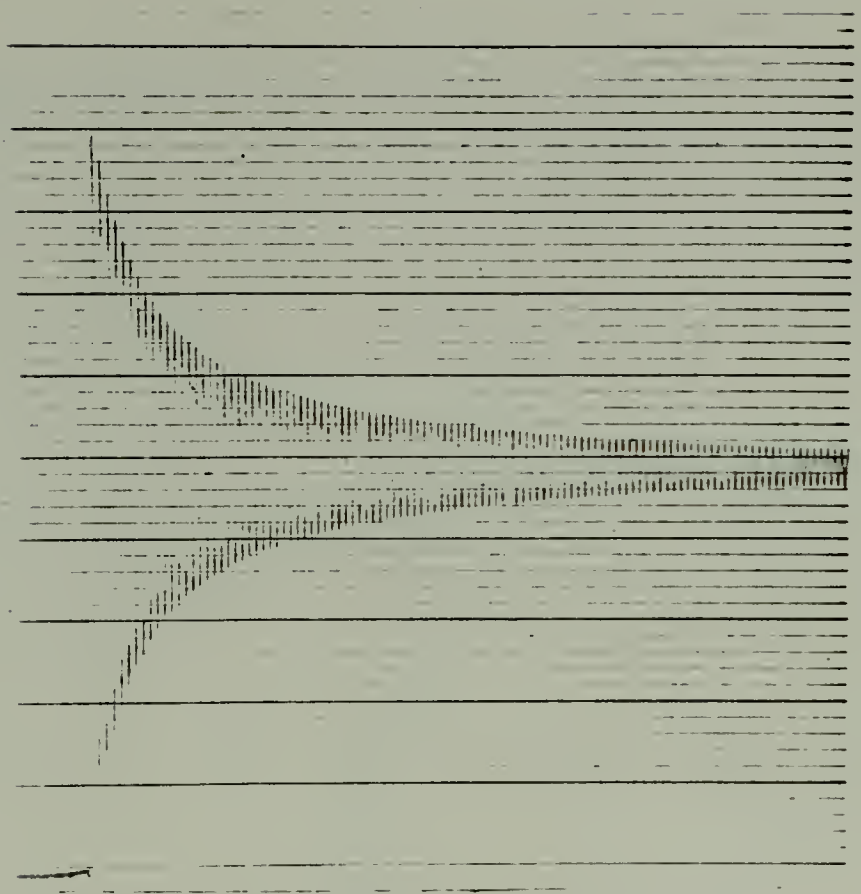

FIGURE 22a. Typical Torsion Pendulum Output for a High Damping Condition

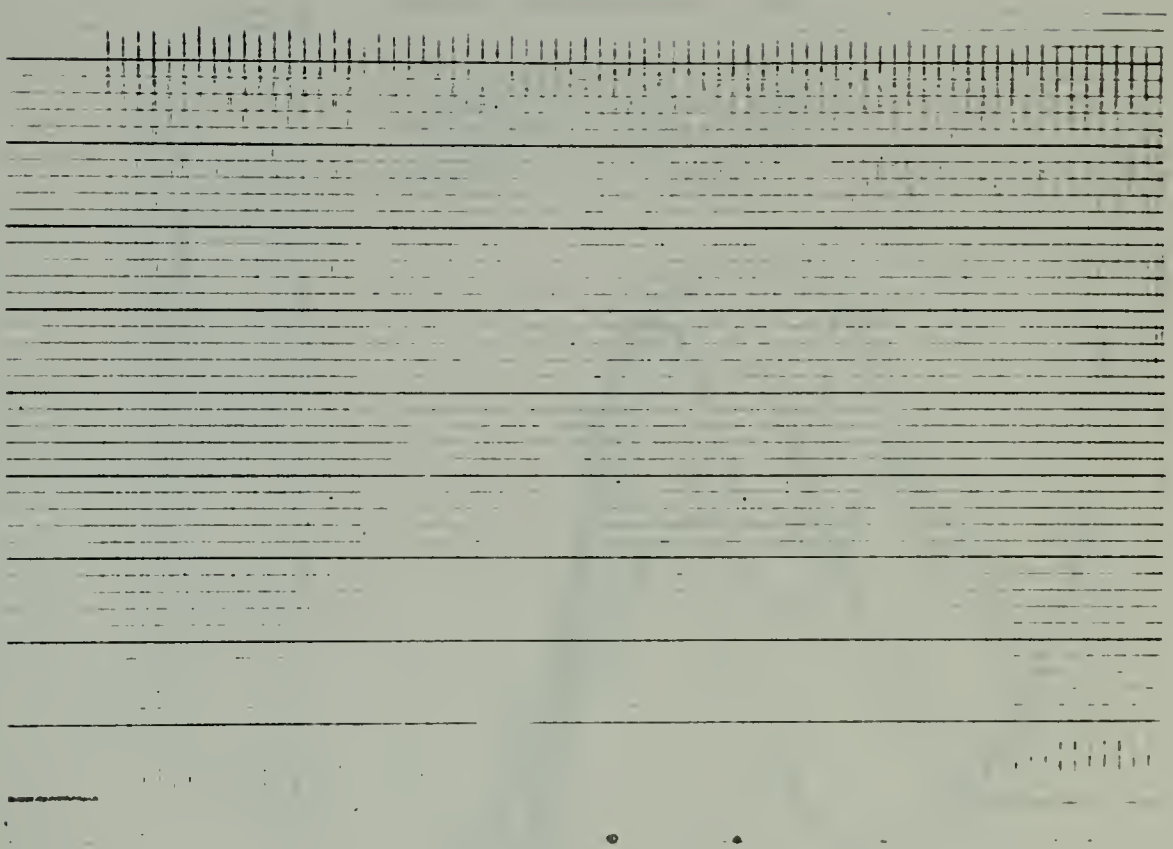

FIGURE 22b. Typical Torsion Pendulum Output for a Low Damping Condition

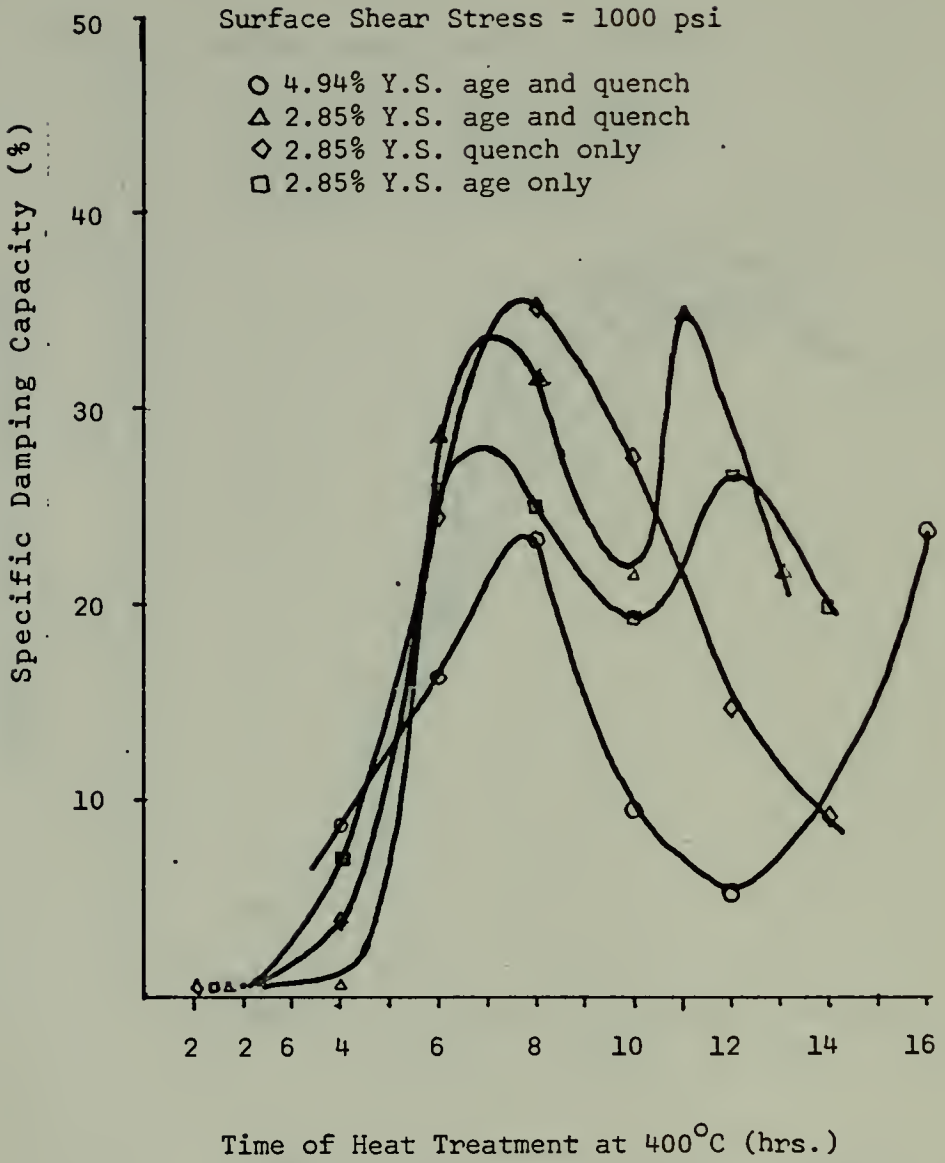

FIGURE 23. Effect of Aging Time on the Damping Capacity of Compression Test Specimens When Measured at 1000 psi Surface Shear Stress

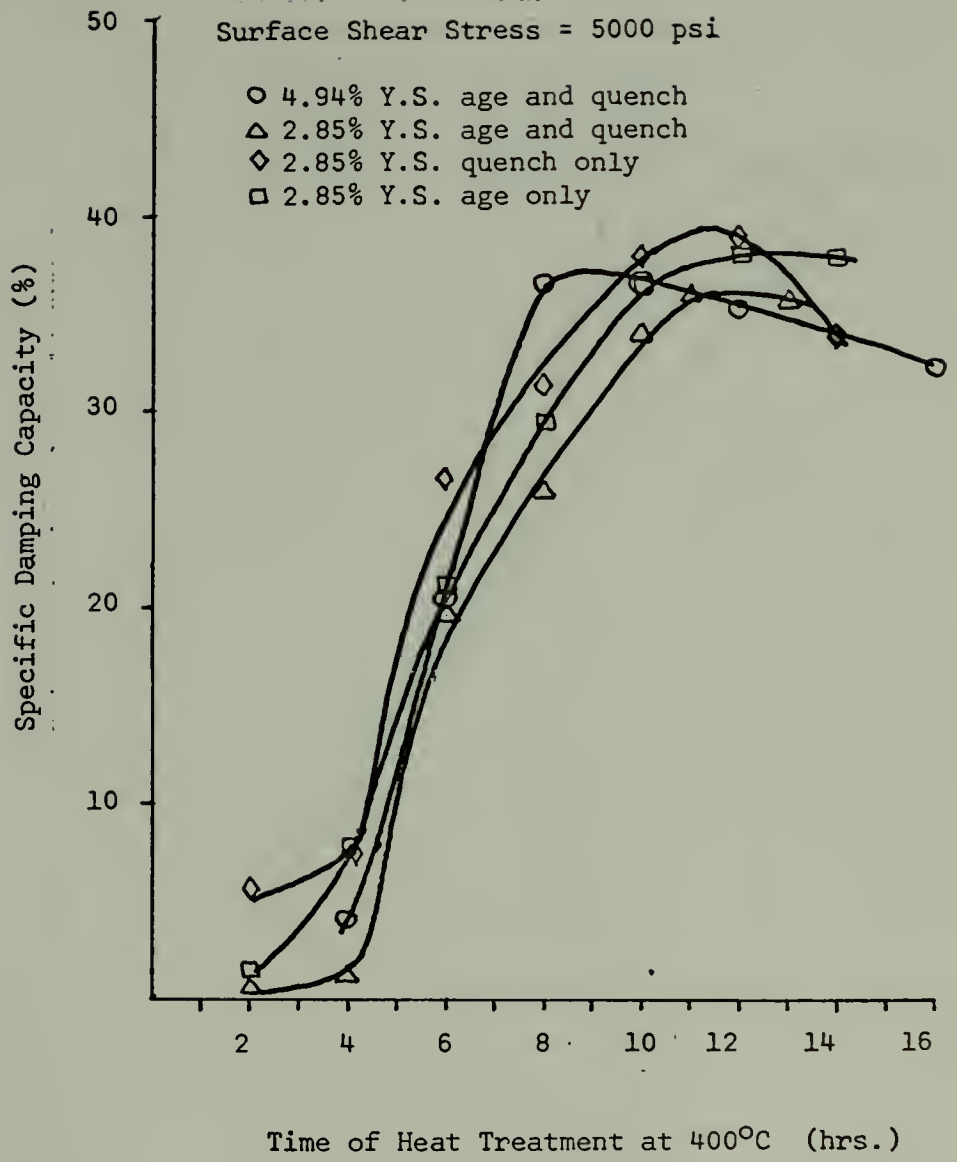

FIGURE 24. Effect of Aging Time on the Damping Capacity of Compression Test Specimens When Measured at 5000 psi Surface Shear Stress

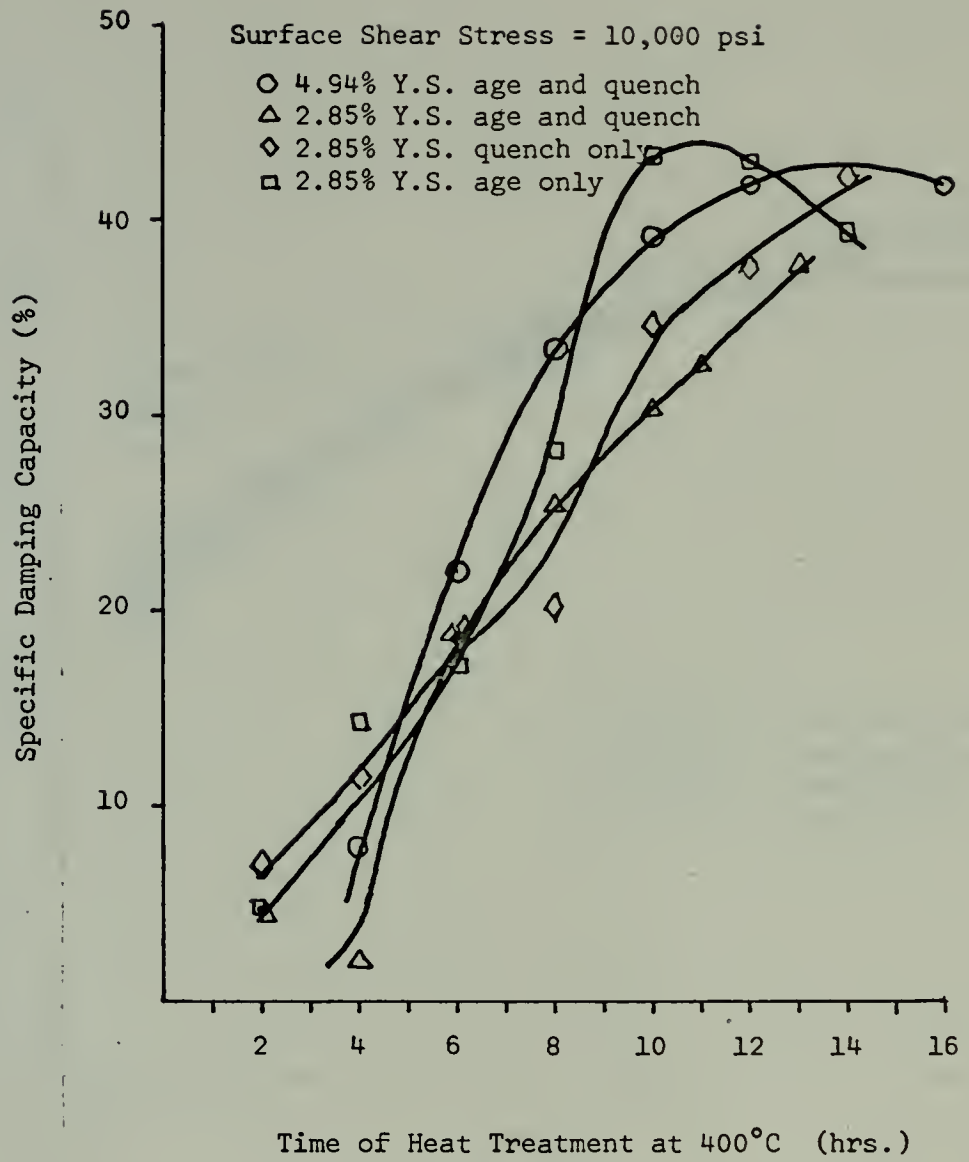

FIGURE 25. Effect of Aging Time on the Damping Capacity of Compression Test Specimens When Measured at 10000 psi Surface Shear Stress

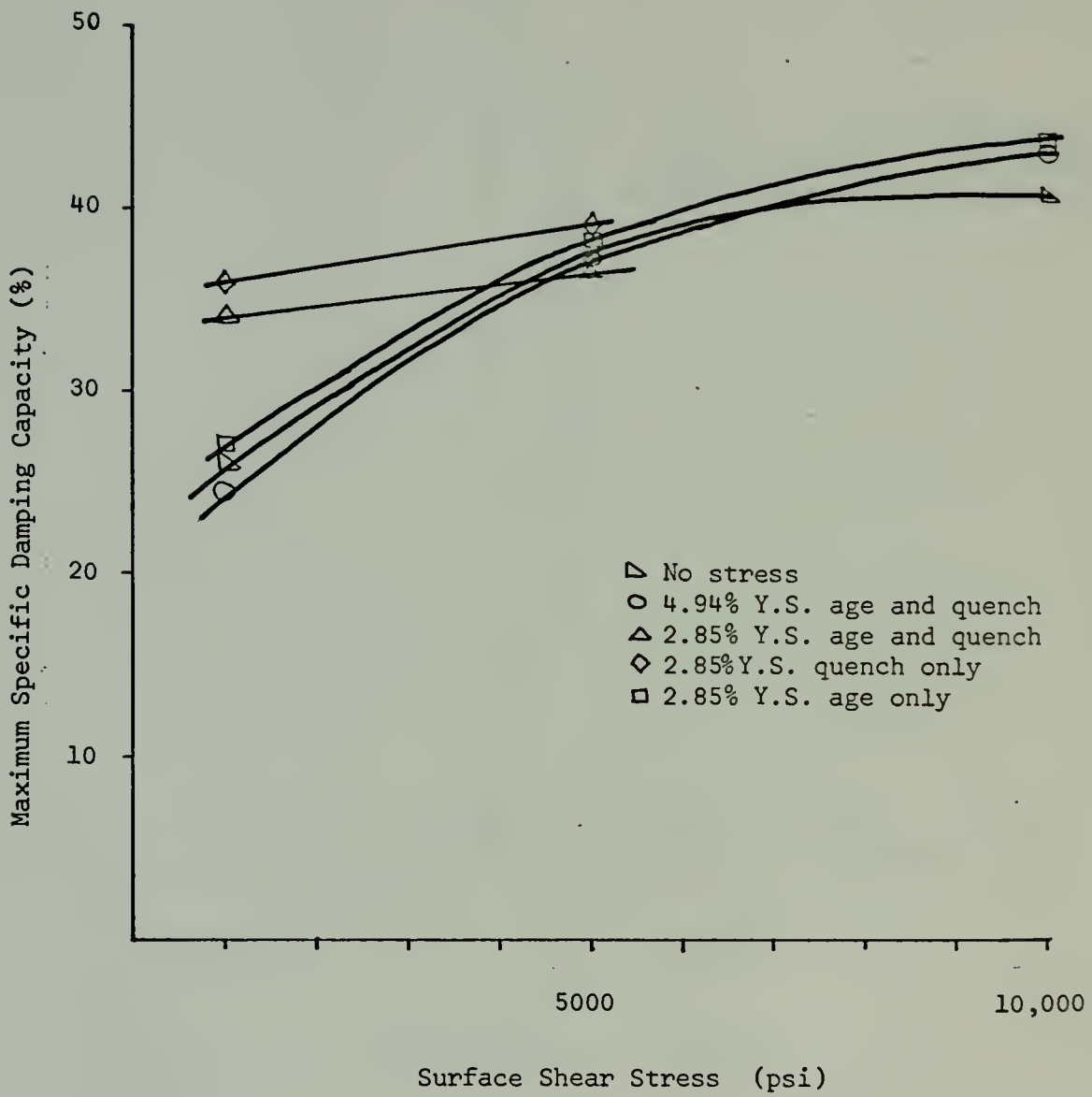

FIGURE 26. Maximum S.D.C. at 400°C for Various Heat Treatments

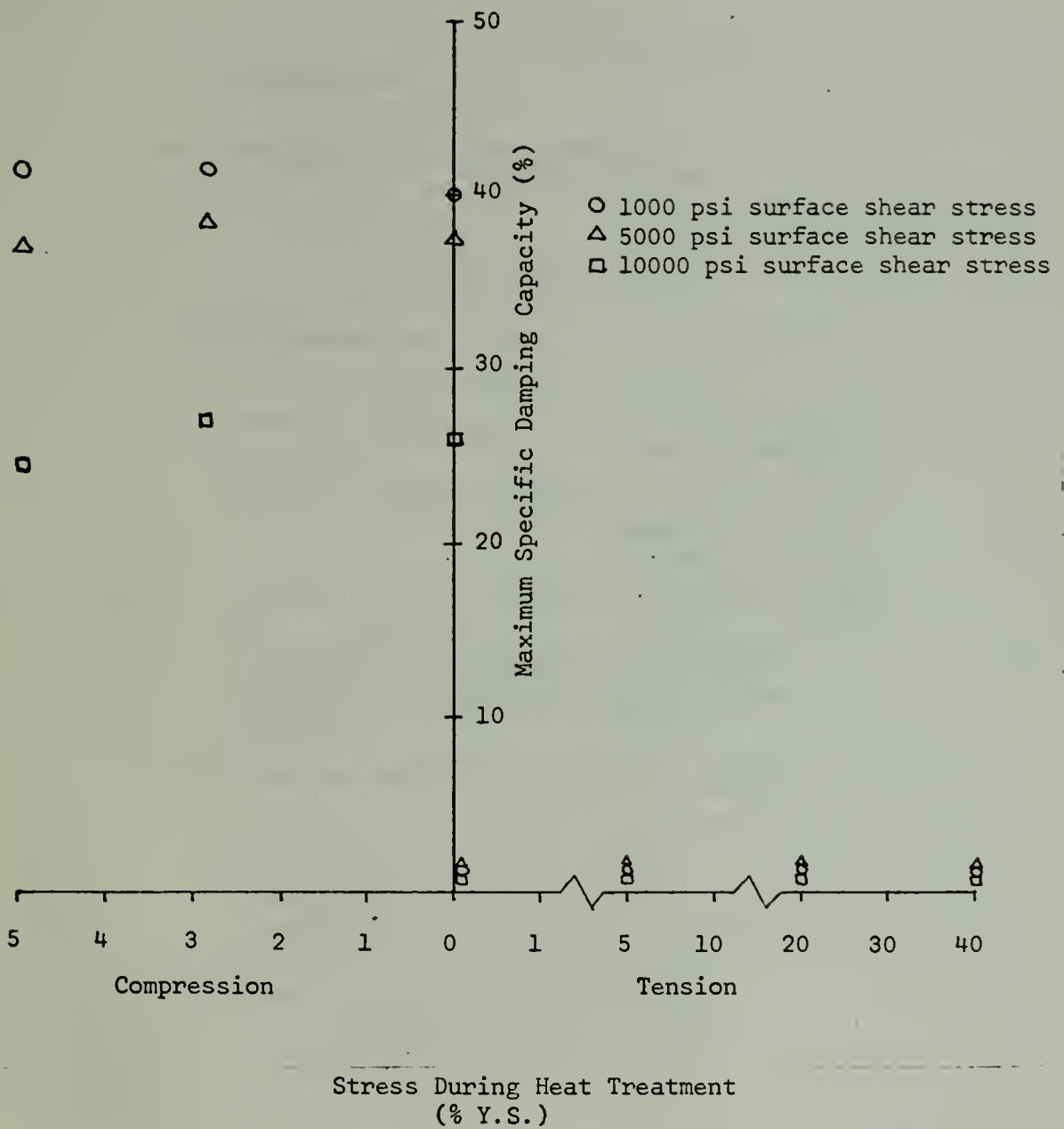

FIGURE 27. Effect of Stress During Heat Treatment on Damping Capacity for Specimens Aged up to 50 Hours at 400°C

Step 1: Solution treatment:

γ_{Mn} ($\cong \alpha_{Cu}$) (Al:FCC)

Step 2: Quench from solution treatment temperature:

If < 80 w/o Mn: γ_{Mn} retained @ room temperature

If > 80 w/o Mn: γ_{Mn} ↓

antiferromagnetic ordering, @ T_N

↓

martensitic transformation @ M_s ($T_N > M_s$)

Step 3: Aging treatment (assuming alloy < 80 w/o Mn) (in two-phase region:

γ_{Mn}(Al:FCC) + α_{Mn} (Al2: complex BCC))

Stage I: γ_{Mn} (initial) γ_{Mn} (Mn-enriched) (matrix) + "ω" (metastable Cu-rich precipitates, 100Å)

Stage II: (more time) γ_{Mn} (Mn-enriched (matrix) + "ω" + α_{Mn} (Widmanstatten precipitate) (small amount)

Stage III: (more time) γ_{Mn} (Mn-depleted) + ~~"ω"~~ dissolves + α_{Mn} (equilibrium amount)

NOTE: The condition of Stage II is typically that leading to optimum damping; Stage III is overaged, i.e. no martensitic transformation of the γ_{Mn} matrix will occur on subsequent quenching - such will occur only if the matrix is conditioned to the necessary Mn-rich state by metastable "ω" precipitation.

Step 4: Quench from the aging treatment (assuming Stage II condition from Step 3 above):

γ_{Mn} (Mn-enriched)	+ "ω" +	α_{Mn} (small amount)
↓ antiferromagnetic ordering @ T_N ↓ martensitic transformation @ M_s	↓ retained ?	↓ retained

NOTE: The martensitic transformation is triggered by the strain associated with the tetragonal distortion (FCC → FCT) of the antiferromagnetic ordering reaction; $T_N > M_s$.

FIGURE 28. Summary of Heat Treatment Effects in Mn-Cu Alloys (from Perkins, Edwards, Hills (26))

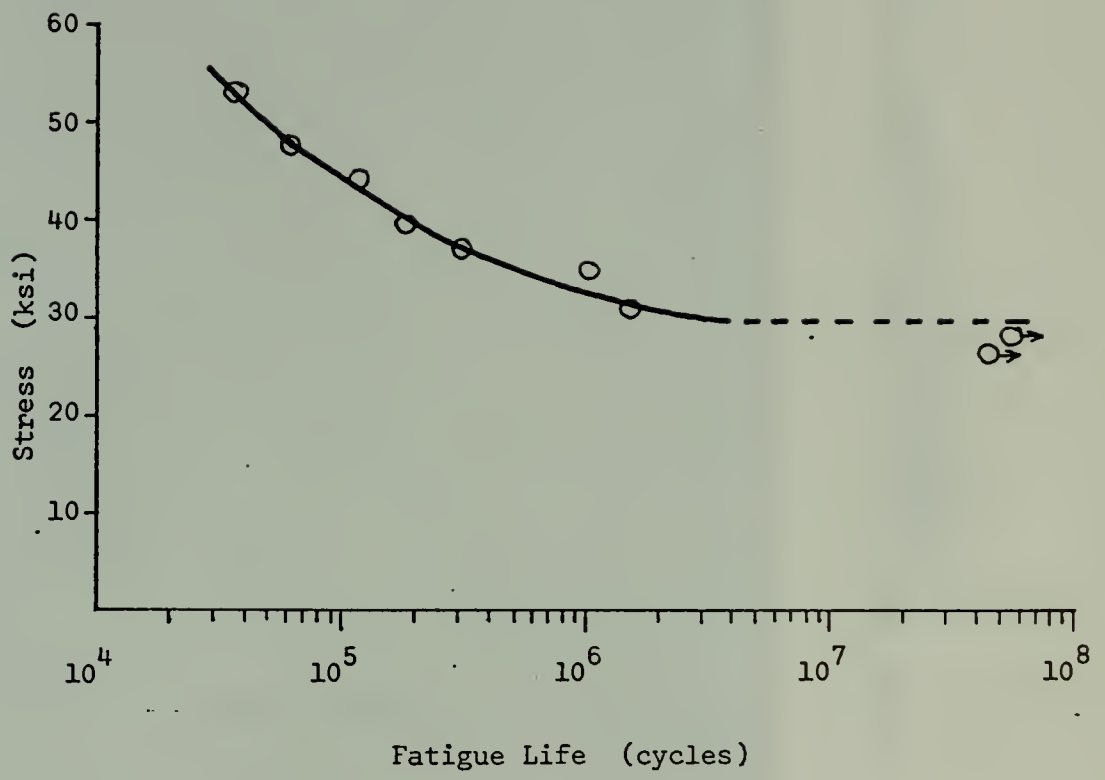

FIGURE 29. S-N Diagram for Incramute Aged 8 Hours at 400°C

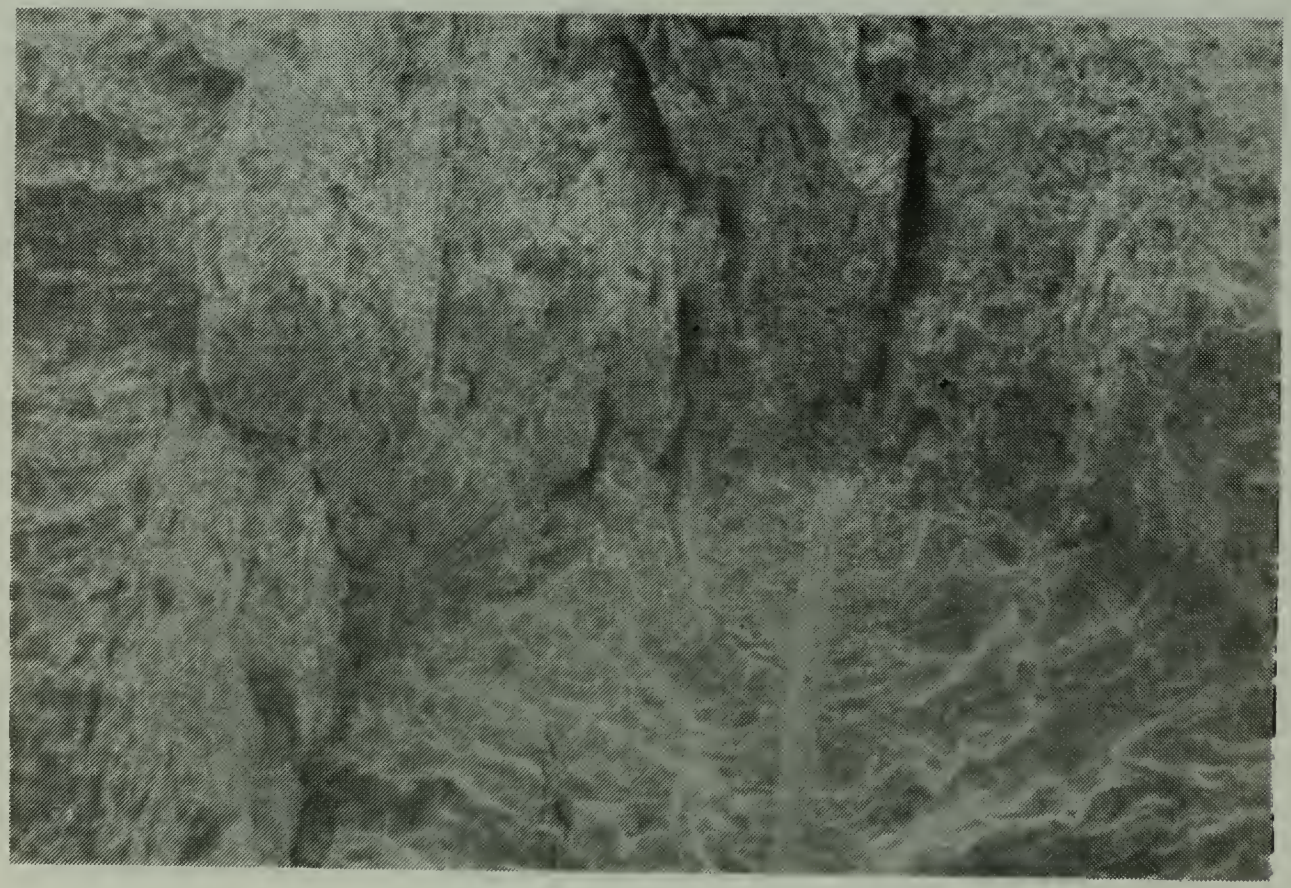

FIGURE 30. Fatigue Fracture Showing Parallel Features and Irregularity of the Surface (22X)

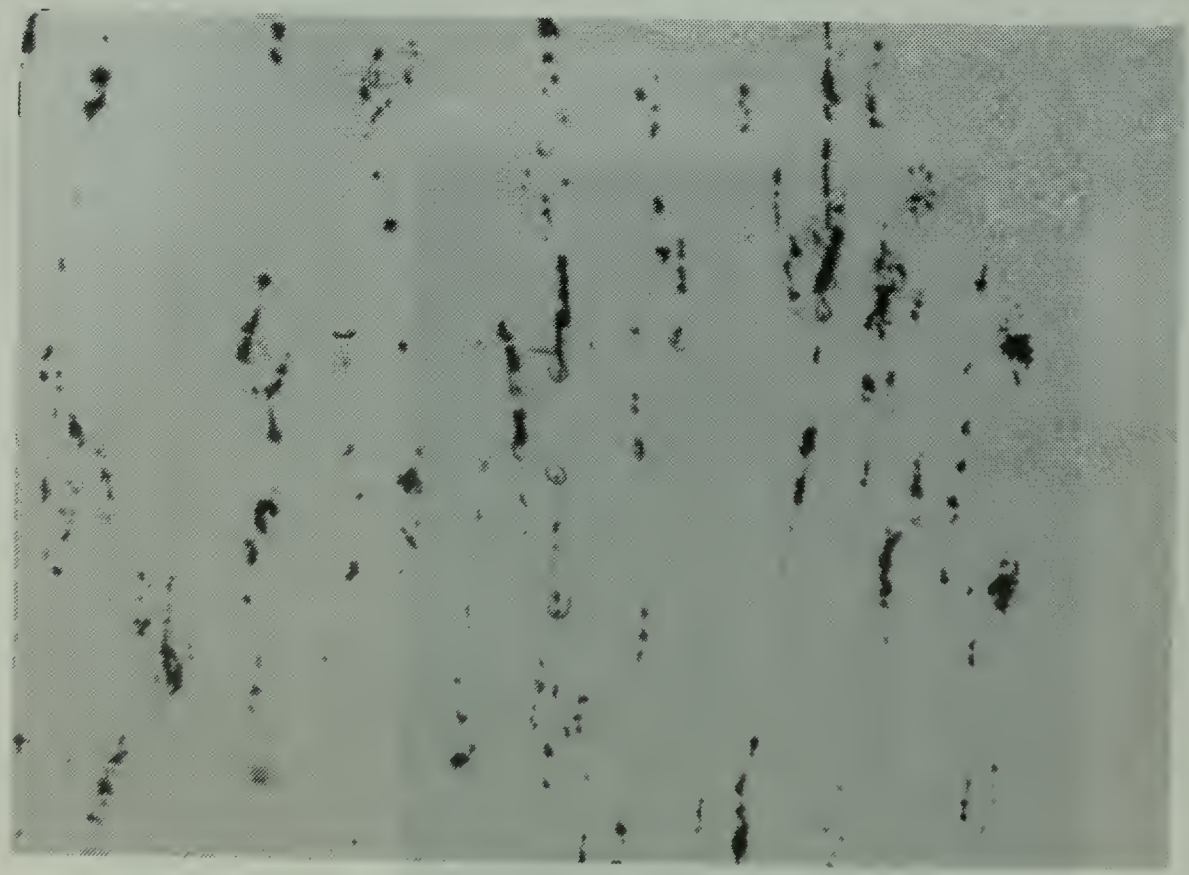

FIGURE 31. Longitudinal Surface of Fatigue Specimen Showing Inclusions and Circular Cracks (265X)

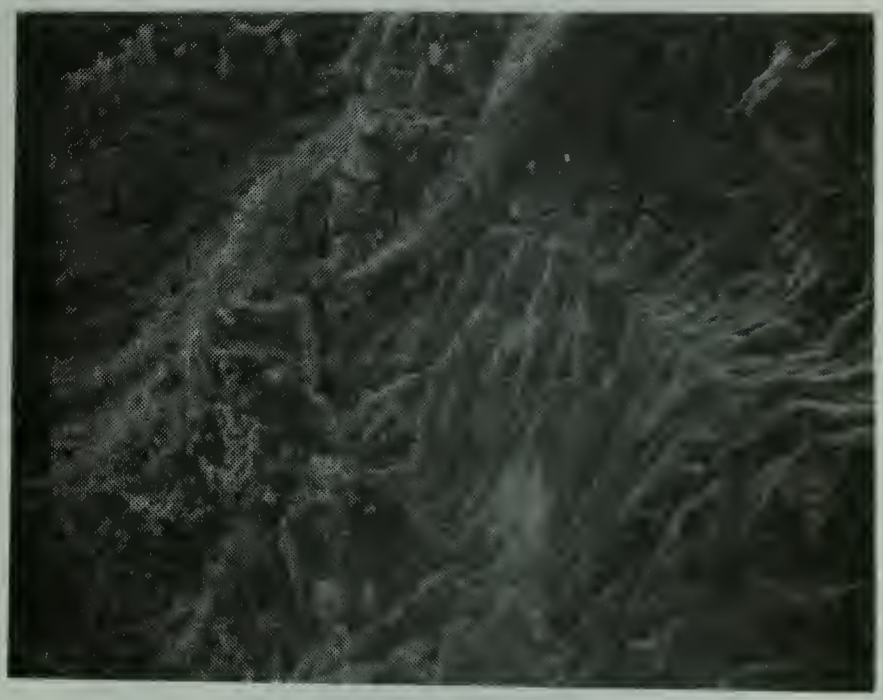

FIGURE 32. Portion of Figure 30 (1568X)

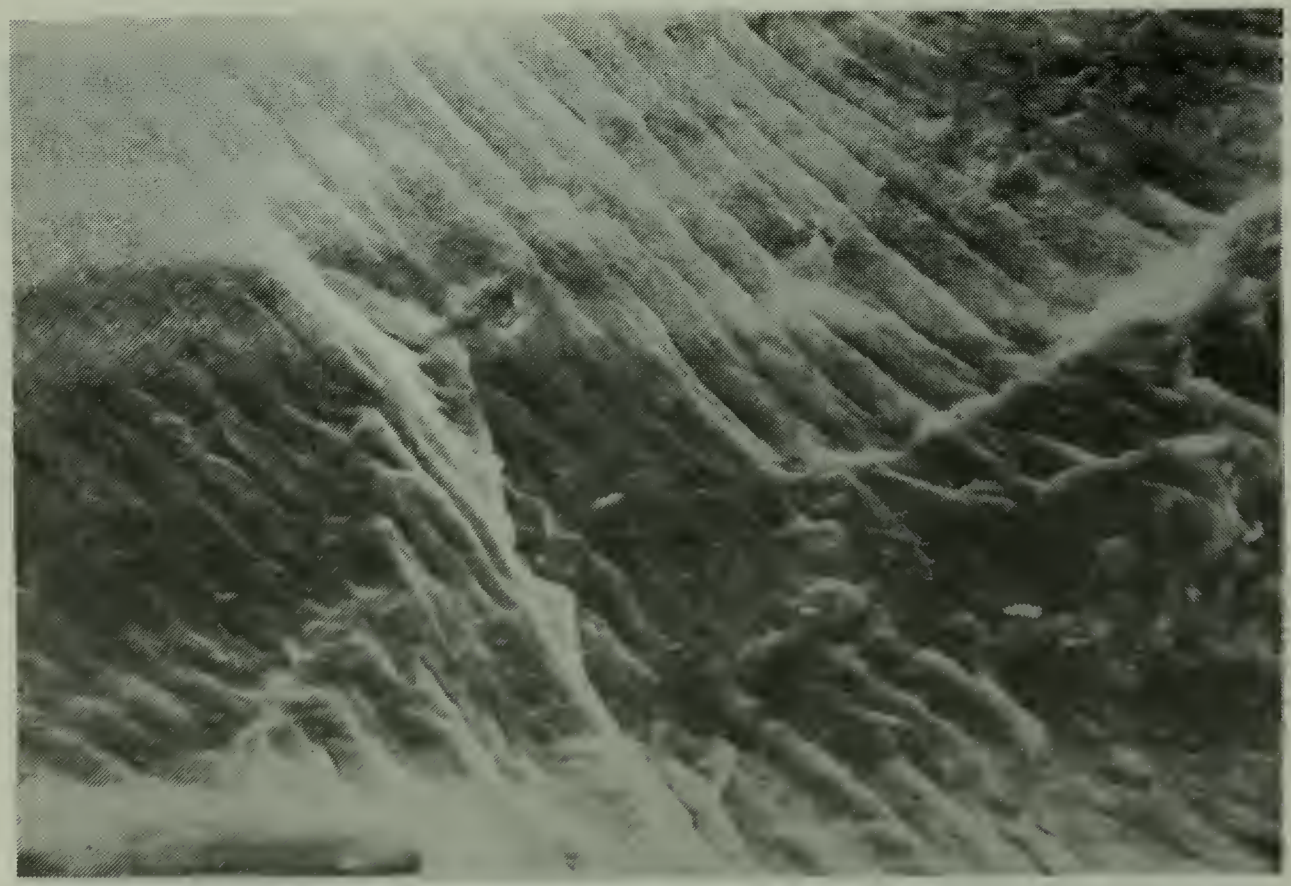

FIGURE 33. Fatigue Striations (3565X)

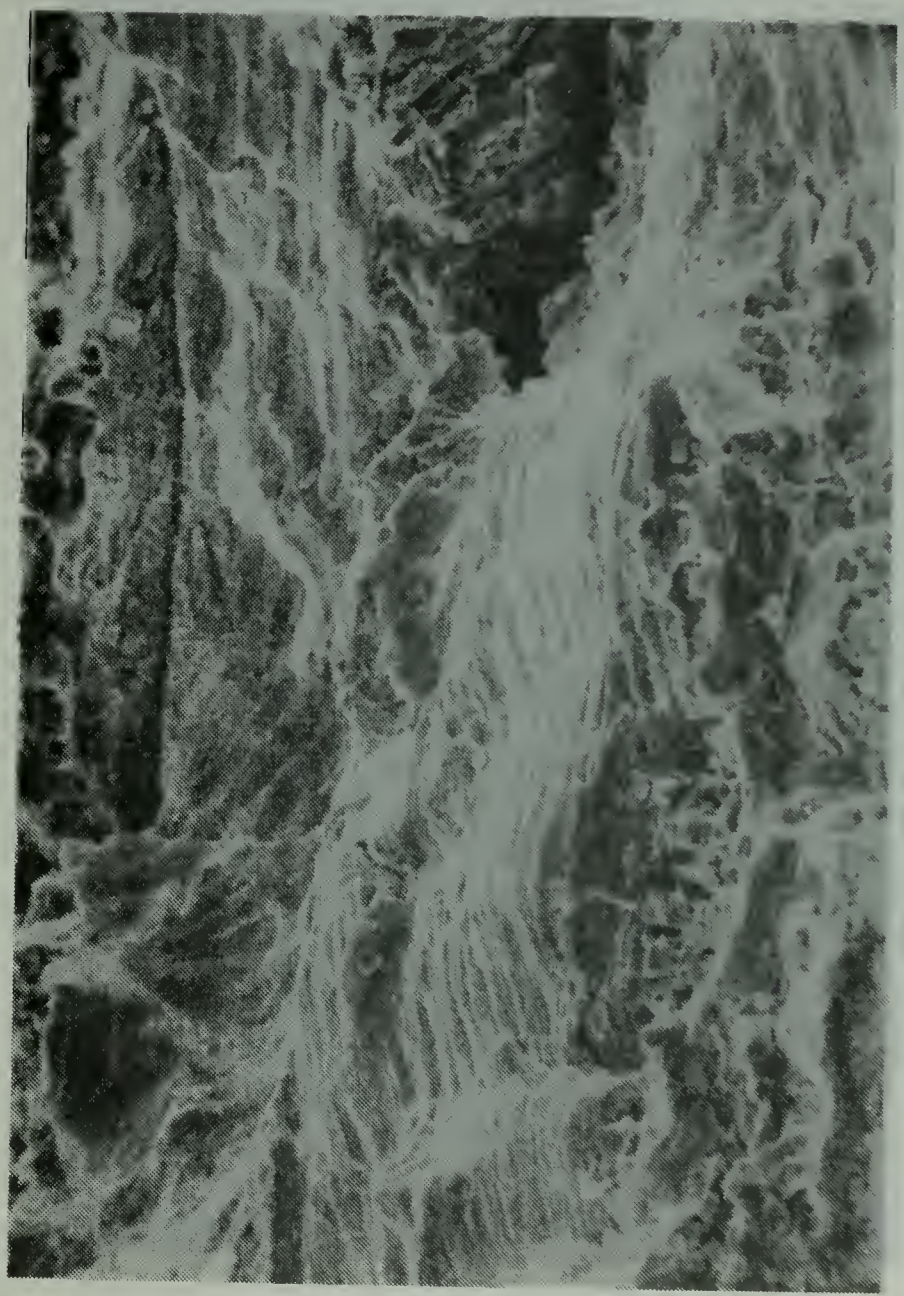

FIGURE 34. Fatigue Striations (891X)

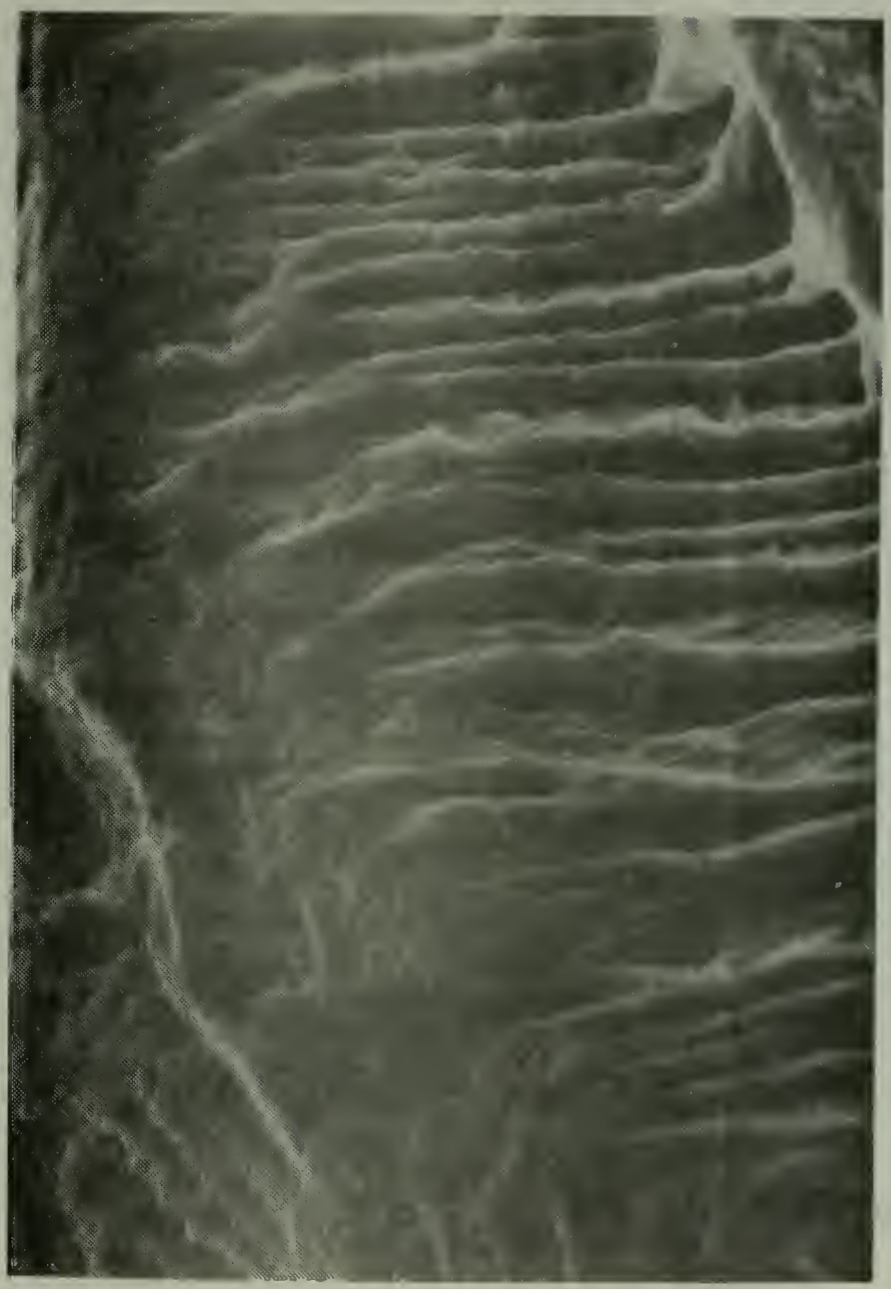

FIGURE 35. Fatigue Striations (3080X)

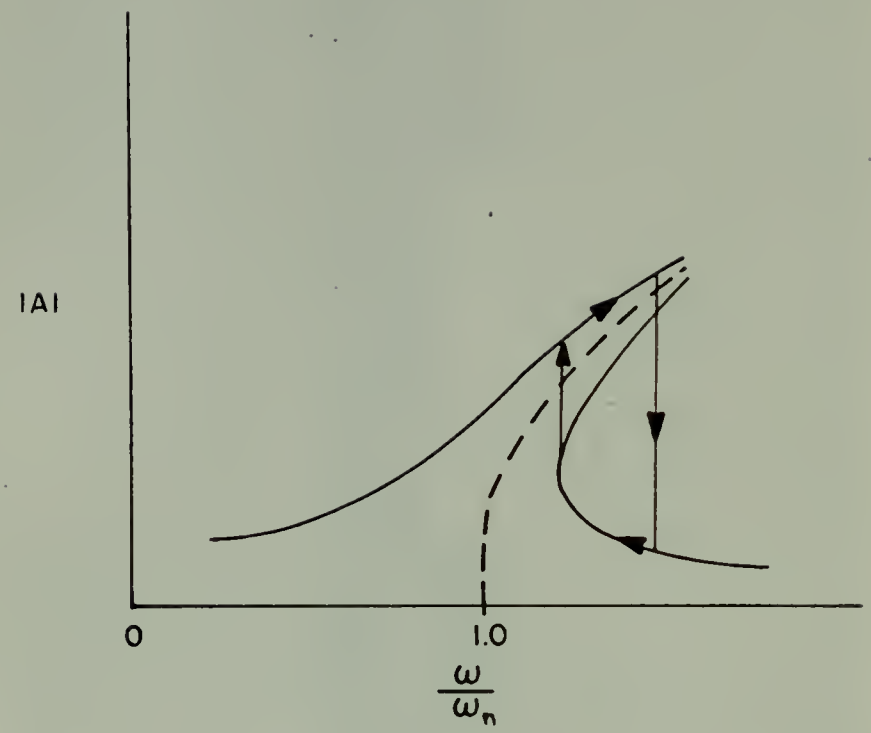

FIGURE 36. Schematic Behavior of a Nonlinear Hardening Spring

FIGURE 37. B&K Instruments, Inc. Complex Modulus Apparatus Type 3930

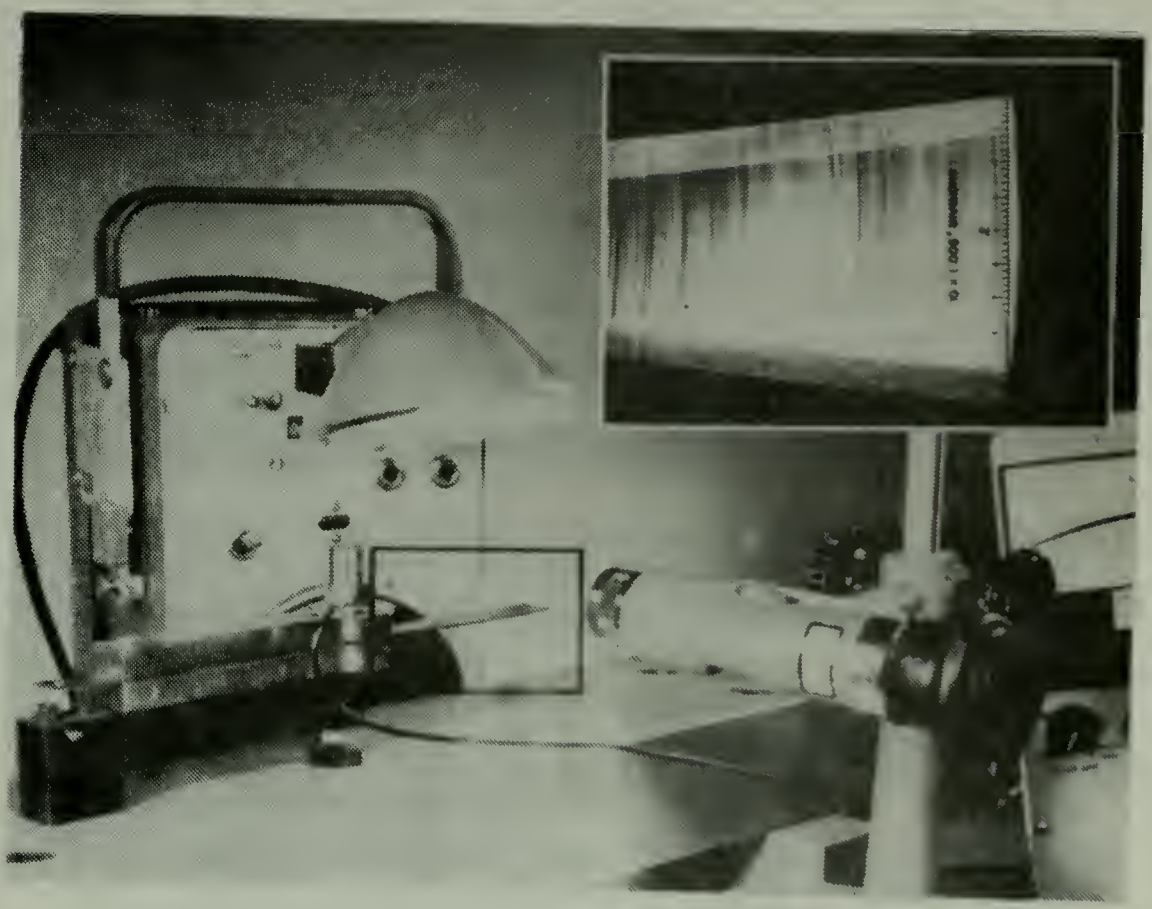

FIGURE 38. Bolt Beranek and Newmann Resonant Dwell Damping Apparatus

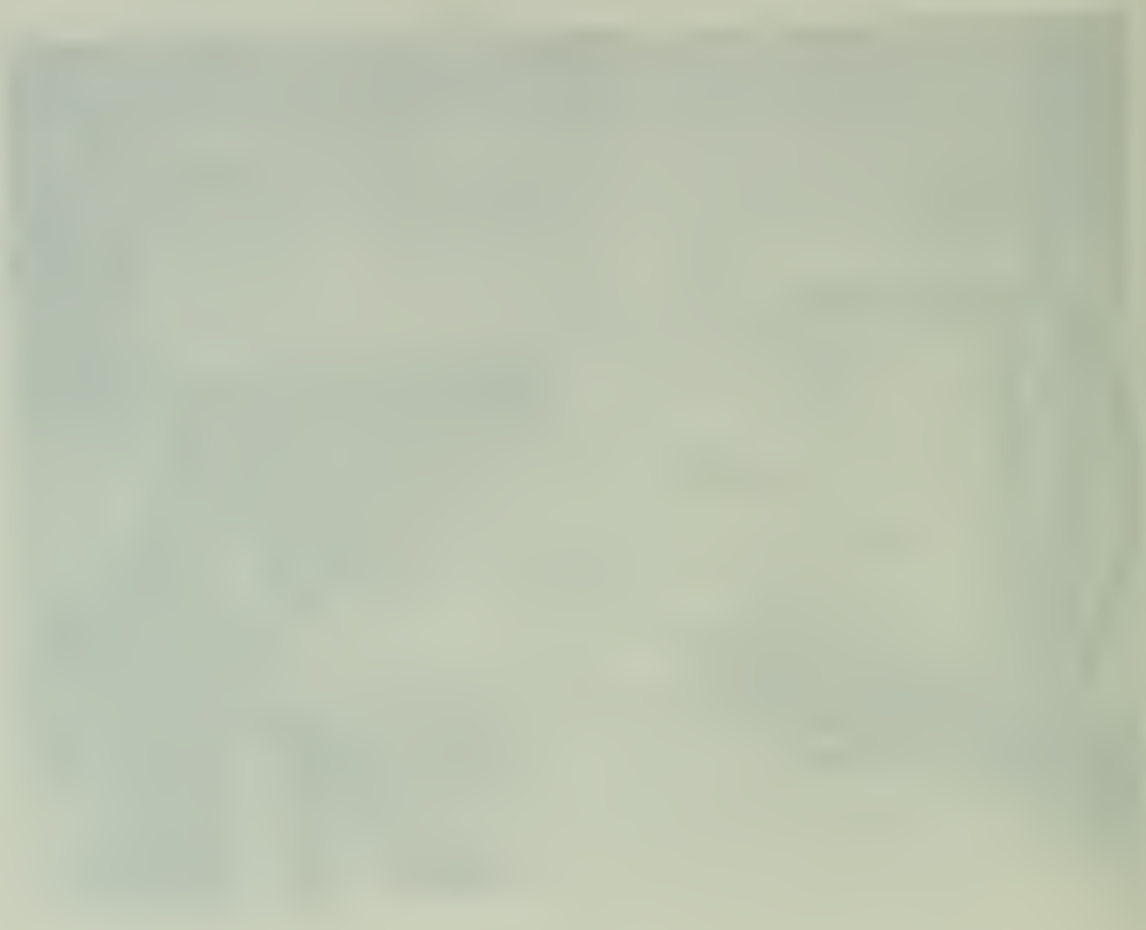

LIST OF REFERENCES

1. Dean, R. S., Potter, E. V., Huber, R. W., Lukens, H. C., "The Damping Capacity of Copper-Manganese Alloys", Transactions of A.S.M., v. 40, p. 355-380, 1948.

2. Dean, R. S., Anderson, C. T., Potter, E. V., "The Alloys of Manganese and Copper: Vibration Damping Capacity", Transactions of A.S.M., v. 29, p.402-414, June 1941.

3. Bureau of Mines Bulletin 624, Manganese-Copper Damping Alloys, Jensen, J. W., Walsh, D. F., 1965.

4. U. S. Naval Engineering Experiment Station, Annapolis, M.D., E.E.S. Report on Test B-2964, Manganese-Copper and Copper-Manganese-Nickel Alloys, Church, A. T., Dec. 23, 1940.

5. U. S. Naval Engineering Experiment Station, Annapolis, M.D., E.E.S. Report on Test C-1824, Cast Manganese-Copper #680 Alloy and Cast Manganese-Copper-Nickel #772 Alloy, Leggett, D. D., May 20, 1947.

6. U. S. Naval Engineering Experiment Station, Annapolis, M.D., E.E.S. Report C-3671, Propeller Material Investigation of High Manganese Alloys for Chicago Development Company, Tydings, H. V., June 16, 1949.

7. U. S. Naval Engineering Experiment Station, Annapolis, M.D., E.E.S. Report 4A(2)066918, High Manganese Alloys for Marine Propellers, Williams, W. L., March 21, 1952.

8. Naval Ship Research and Development Center, Annapolis Laboratory, Report 8-975, Corrosion Behavior of Manganese-Copper-Vanadium Alloy, Nov. 16, 1971 (document For Official Use Only)

9. Naval Ship Research and Development Center, Annapolis Laboratory, Report 3236, Development of Improved Alloys for Navy Ships Propellers. Phase I - High Damping Alloys, Czyryca, E. J., Vassilaros, M. G., June 1971.

10. Naval Ship Research and Development Center, Annapolis Laboratory, Report 28-511, Mechanical Properties of Lidrunel 90S Cast Propeller Alloy (Interim Report), December 1, 1972 (document For Official Use Only)

11. Reference deleted

12. U. S. Naval Engineering Experiment Station, Annapolis, M.D., E.E.S. Report 040016D, Investigation of Materials for Propulsion Gears: An Evaluation of 80-20 Manganese-Copper Alloy, Greenert, W. J., February 29, 1956.

13. Hedley, J. A., "The Mechanism of Damping in Manganese-Copper Alloys", Metal Science Journal, v. 2, p.129-137, July 1968.

14. Butler, E. P., Kelley, P. M., "High Damping Capacity Manganese-Copper Alloys. Pt. 2. The Effect of Storage and of Deformation on the Damping Capacity of 70/30 Mn-Cu Alloy", Transactions of the Metallurgical Society of AIME, v. 242, p.2107-2109, October 1968.

15. Butler, E. P., Kelley, P. M., "High Damping Capacity Manganese-Copper Alloys. Pt. 1. Metallography", Transactions of the Metallurgical Society of AIME, v. 242, p.2099-2106, October 1968.

16. Langham, J. M., "A New High-Damping Alloy", Foundry Trade Journal, p. 989-998, June 6, 1968.

17. Dean, R. S., Long, C. R., Graham, T. R., Roberson, A.A., Armantrout, C. E., "The Alpha Solid Solution Area of the Copper-Manganese-Aluminum System", Transactions of the AIME, v. 171, p.70-88, 1947.

18. Huhn, W. P., American Potash and Chemical Corporation, Private Communication dated April 28, 1970.

19. Birchon, D., Bromley, E. E., Healey, D., "Mechanism of Energy Dissipation in High-Damping-Capacity Manganese-Copper Alloys", Metal Science Journal, v. 2, p.41-46, March 1968.

20. Perkins, J. "Lattice Transformations Related to Unique Mechanical Effects", Metallurgical Transactions, v. 4, p.2709-2721, 1973.

21. Bureau of Mines Report of Investigations 5853, Fatigue Properties of Manganese-Copper Damping Alloys, Jensen, J. W., Schwaneke, A. E., Walsh, D. F., 1961.

22. Farthing, T. W., "Manganese-Copper - The Silent Metal", Engineering, p.632-633, November 13, 1964.

23. Olin Metals Research Labs, Final Report, INCRA Project No. 205, Incramute I - Processing and Properties, July 1973.

24. International Copper Research Association, Inc., Properties of Incramute High-Damping Alloy, June 1973.

25. Birchon, D., "High Damping Alloys: Part 1", Engineering Materials and Design, v. 7, p.606-608, September 1964.

26. Naval Postgraduate School Report NPS-59Ps74061, Materials Approaches to Ship Silencing, Perkins, A. J., Edwards, G. R., Hills, N. A., June 1974.

27. National Aeronautics and Space Administration, NASA TN D-109, Effects of Creep Stress on Particulate Aluminum-Copper Alloys, Underwood, E. E., Manning, G. K., September 1959.

28. Nileshwar, V. B., "Some Observations on the Kinetics of Aging Reactions During Creep of Aluminum Alloys", Journal of the Institute of Metals, v. 92, p.241-245, 1964.

29. Patel, J. R., Cohen, M., "Criterion for the Action of Applied Stress in the Martensitic Transformation", Acta Metallurgica, v. 1, p.531-538, September 1953.

30. Bert, C. W., "Material Damping: An Introductory Review of Mathematical Models, Measures and Experimental Techniques", Journal of Sound and Vibration, v. 29, p.129-153, 1973.

31. Bureau of Mines Report of Investigations 5441, Damping Capacity - Its Measurement and Significance, Jensen, J. W., Walsh, D. F., 1965.

32. Jensen, J. W., "A Torsion Pendulum of Improved Design for Measuring Damping Capacity", The Review of Scientific Instruments, v. 23, no. 8, p.397-401, August 1952.

33. Kline, S. J., McClintock, F. A., "Describing Uncertainties in Single-Sample Experiments", Mechanical Engineering, p.3-8, January 1953.

34. James, D. W., "High Damping Metals for Engineering Applications", Materials Science and Engineering, v. 4, p.1-8, 1969.

35. Basinski, Z. S., Christian, J. W., "The Cubic-Tetragonal Transformation in Mn-Cu Alloys", Journal of the Institute of Metals, v. 80, p.659-666, 1951-1952.

INITIAL DISTRIBUTION LIST

		No. Copies
1.	Defense Documentation Center Cameron Station Alexandria, Virginia 22314	2
2.	Library, Code 0212 Naval Postgraduate School Monterey, California 93940	2
3.	Chairman, Code 59 Department of Mechanical Engineering Naval Postgraduate School Monterey, California 93940	2
4.	Capt. L. H. Beck, Code 037 Naval Ship Systems Command Ship Silencing Program Washington, D.C. 20350	1
5.	Mr. S. M. Blazek Naval Ship Systems Command Ship Silencing Program Washington, D.C. 20350	1
6.	Mr. E. J. Czyryca Naval Ship Research and Development Laboratory Annapolis, Maryland 21402	1
7.	Professor A. J. Perkins Department of Mechanical Engineering Naval Postgraduate School Monterey, California 93940	5
8.	Professor G. R. Edwards Department of Mechanical Engineering Naval Postgraduate School Monterey, California 93940	5
9.	Lt. N. A. Hills SMC 1829 Naval Postgraduate School Monterey, California 93940	5

155088
Thesis
H5336 Hills
c.1
A study of the influence of stress and temperature on the damping capacity of Mn-Cu alloys for ship silencing applications.